Guidelines for Studying Diverse Types of Compound Weather and Climate Events

Emanuele Bevacqua[1,2] , **Carlo De Michele**[3] , **Colin Manning**[4] , **Anaïs Couasnon**[5] , **Andreia F. S. Ribeiro**[6,7] , **Alexandre M. Ramos**[7] , **Edoardo Vignotto**[8] , **Ana Bastos**[9] , **Suzana Blesić**[10] , **Fabrizio Durante**[11] , **John Hillier**[12] , **Sérgio C. Oliveira**[13] , **Joaquim G. Pinto**[14] , **Elisa Ragno**[15] , **Pauline Rivoire**[16] , **Kate Saunders**[17] , **Karin van der Wiel**[18] , **Wenyan Wu**[19] , **Tianyi Zhang**[20] , and **Jakob Zscheischler**[1,21,22]

[1]Department of Computational Hydrosystems, Helmholtz Centre for Environmental Research—UFZ, Leipzig, Germany, [2]Department of Meteorology, University of Reading, Reading, UK, [3]Department of Civil and Environmental Engineering, Politecnico di Milano, Milano, Italy, [4]School of Civil Engineering and Geosciences, Newcastle University, Newcastle upon Tyne, UK, [5]Institute for Environmental Studies, Vrije Universiteit Amsterdam, Amsterdam, The Netherlands, [6]Institute for Atmospheric and Climate Science, ETH Zurich, Zurich, Switzerland, [7]Instituto Dom Luiz (IDL), Faculdade de Ciências, Universidade de Lisboa, Lisboa, Portugal, [8]Research Center for Statistics, University of Geneva, Geneva, Switzerland, [9]Department of Biogeochemical Integration, Max Planck Institute for Biogeochemistry, Jena, Germany, [10]University of Belgrade and Center for Participatory Science, Institute for Medical Research, Belgrade, Serbia, [11]Department of Economic Sciences, University of Salento, Lecce, Italy, [12]Geography, Loughborough University, Loughborough, UK, [13]Centre for Geographical Studies and Associated Laboratory TERRA, Institute of Geography and Spatial Planning, Universidade de Lisboa, Lisboa, Portugal, [14]Institute of Meteorology and Climate Research, Karlsruhe Institute of Technology, Karlsruhe, Germany, [15]Faculty of Civil Engineering and Geosciences, Delft University of Technology, Delft, The Netherlands, [16]Oeschger Centre for Climate Change Research and Institute of Geography, University of Bern, Bern, Switzerland, [17]School of Mathematical Sciences, Queensland University of Technology, Brisbane, QL, Australia, [18]Royal Netherlands Meteorological Institute (KNMI), De Bilt, The Netherlands, [19]Department of Infrastructure Engineering, Faculty of Engineering and Information Technology, The University of Melbourne, Melbourne, VIC, Australia, [20]State Key Laboratory of Atmospheric Boundary Layer Physics and Atmospheric Chemistry, Institute of Atmospheric Physics, Chinese Academy of Sciences, Beijing, China, [21]Climate and Environmental Physics, University of Bern, Bern, Switzerland, [22]Oeschger Centre for Climate Change Research, University of Bern, Bern, Switzerland

Abstract Compound weather and climate events are combinations of climate drivers and/or hazards that contribute to societal or environmental risk. Studying compound events often requires a multidisciplinary approach combining domain knowledge of the underlying processes with, for example, statistical methods and climate model outputs. Recently, to aid the development of research on compound events, four compound event types were introduced, namely (a) *preconditioned*, (b) *multivariate*, (c) *temporally compounding*, and (d) *spatially compounding* events. However, guidelines on how to study these types of events are still lacking. Here, we consider four case studies, each associated with a specific event type and a research question, to illustrate how the key elements of compound events (e.g., analytical tools and relevant physical effects) can be identified. These case studies show that (a) impacts on crops from hot and dry summers can be exacerbated by preconditioning effects of dry and bright springs. (b) Assessing compound coastal flooding in Perth (Australia) requires considering the dynamics of a non-stationary multivariate process. For instance, future mean sea-level rise will lead to the emergence of concurrent coastal and fluvial extremes, enhancing compound flooding risk. (c) In Portugal, deep-landslides are often caused by temporal clusters of moderate precipitation events. Finally, (d) crop yield failures in France and Germany are strongly correlated, threatening European food security through spatially compounding effects. These analyses allow for identifying general recommendations for studying compound events. Overall, our insights can serve as a blueprint for compound event analysis across disciplines and sectors.

Plain Language Summary Many societal and environmental impacts from events such as droughts and storms arise from a combination of weather and climate factors referred to as a *compound event*. Considering the complex nature of these high-impact events is crucial for an accurate assessment of climate-related risk, for example to develop adaptation and emergency preparedness strategies. However, compound event research has emerged only recently, therefore our ability to analyze these events is still

Pauline Rivoire, Kate Saunders, Wenyan Wu, Jakob Zscheischler

Project Administration: Emanuele Bevacqua, Carlo De Michele, Colin Manning, Anaïs Couasnon, Alexandre M. Ramos, Edoardo Vignotto, Jakob Zscheischler

Resources: Alexandre M. Ramos, Ana Bastos, Sérgio C. Oliveira, Joaquim G. Pinto, Karin Wiel, Wenyan Wu, Tianyi Zhang

Supervision: Jakob Zscheischler

Writing – original draft: Emanuele Bevacqua, Carlo De Michele, Colin Manning, Anaïs Couasnon, Jakob Zscheischler

Writing – review & editing: Emanuele Bevacqua, Carlo De Michele, Colin Manning, Anaïs Couasnon, Andreia F. S. Ribeiro, Alexandre M. Ramos, Edoardo Vignotto, Ana Bastos, Suzana Blesić, Fabrizio Durante, John Hillier, Sérgio C. Oliveira, Joaquim G. Pinto, Elisa Ragno, Pauline Rivoire, Kate Saunders, Karin Wiel, Wenyan Wu, Tianyi Zhang, Jakob Zscheischler

limited. In practice, studying compound events is a challenging task, which often requires interaction between experts across multiple disciplines. Recently, compound events were divided into four types to aid the framing of research on this topic, but guidelines on how to study these four types are missing. Here, we take a pragmatic approach and—focusing on case studies of different compound event types— illustrate how to address specific research questions that could be of interest to users. The results allow identifying recommendations for compound event analyses. Furthermore, through the case studies, we highlight the relevance that compounding effects have for the occurrence of landslides, flooding, vegetation impacts, and crop failures. The guidelines emerged from this work will assist the development of compound event analysis across disciplines and sectors.

1. Introduction

Many high-impact weather and climate events arise from a combination of multiple drivers and/or hazards such as droughts, heatwaves, heavy precipitation, and storms (Zscheischler et al., 2018). Therefore, understanding and ultimately modeling the complex nature of such *compound events* is essential for accurately assessing weather- and climate-induced risks. However, although the inherently complex nature of the environmental system has always threatened societies via combined weather and climate processes, compound-event-oriented research has emerged only recently. As a result, our ability to identify, understand, and model compound events is still in its infancy (Zscheischler et al., 2020).

Studying compound events is a complex task, which often requires a multidisciplinary approach involving the understanding of the underlying physical processes beyond the impact, climate, and weather elements, and advanced process-based and statistical modeling (Bevacqua et al., 2017). Consequently, for users, it is often difficult to identify the key elements (i.e., physical variables, relevant spatial and temporal scales as well as suitable analysis tools and datasets) necessary to address a given compound event-related research question. In this context, a common framework for compound event analysis could be very helpful to users. However, developing such a framework is challenging because the *physical elements* that constitute a compound event can combine in a myriad of ways, for example across multiple spatiotemporal scales (Messori et al., 2021). In particular, these physical elements are (a) the societal or environmental *impacts* (e.g., damages to railway infrastructures or crop failure), (b) the climate-related *hazards* (e.g., a heatwave or flood), causing the impact itself, (c) the *drivers* of the hazards (e.g., a long-lasting atmospheric blocking causing a heatwave), and (d) the *modulators* of the drivers (e.g., an anomalous state of the atmospheric circulation during a season). Finally, (e) climate change can influence modulators, drivers and hazards (Zscheischler et al., 2020). The multiple possible combinations of these physical elements result in distinct event types whose physical understanding, modeling, and analysis require different approaches, methods, and datasets.

Recently, to aid the framing and development of new research on compound events, four distinct classes of event types were proposed (Zscheischler et al., 2020). (a) *Preconditioned events* refer to a situation where a climate or weather background precondition can enhance the impact triggered by one or more hazards; (b) *Multivariate events* can result in impacts due to concurrent drivers and/or hazards at about the same location; (c) *Temporally compounding events*, which can lead to impacts due to a sequence of hazards; (d) *Spatially compounding events*, which can lead to aggregated impacts as a result of hazards occurring in multiple connected locations. Importantly, this typology has the potential for enabling the development of user-friendly practical guidelines for compound event analysis, which would be tailored to specific compound event types.

In this study, we contribute to the development of such user-friendly guidelines, focusing on the weather/ climate component of impacts, that is, we focus on hazards that can potentially cause impacts to vulnerable populations and assets. We illustrate how to address specific research questions for four case studies selected to represent the four different compound event types. Such a pragmatic approach allows for illustrating and discussing how to identify the key elements of compound events in a context that is plausible for users. While the presented insights will be somewhat specific for the selected four case studies, considering four event types allows exploring a relatively wide range of methods and physical characteristics that will be used to provide general guidance for compound event analysis.
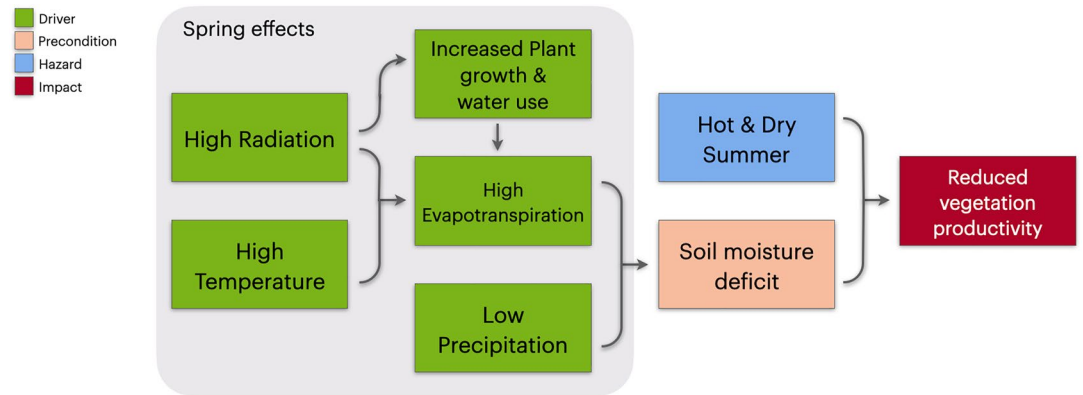
Figure 1. Physical elements of vegetation impacts arising from a combination of summertime hot and dry conditions and soil moisture precondition driven by springtime effects (see details in Section 2.1). Arrows indicate causal links. Note that while wind and humidity also modulate evapotranspiration (ET), they are not shown here for simplicity.

The four considered compound events are summertime vegetation impacts from springtime weather (a preconditioned event), projections of compound coastal flooding (multivariate), landslides from precipitation clustering (temporally compounding), and concurrent crop failures across different European countries (spatially compounding). In each of the following four subsections, we first introduce the case study and associated research question. We then identify the key elements of the compound events including tools that can be used to address the research question at hand. At the end of each subsection, we identify compound events that could be investigated with tools similar to those considered here. In a final section, we discuss common aspects and guidelines emerging from the four case studies.

2. Preconditioned Event: Springtime Weather Modulates Summertime Vegetation Impacts

### 2.1. Introduction and Research Question

The negative impact of hot and dry summers on vegetation productivity can be exacerbated by a pre-existing soil moisture deficit arising from meteorological drought and an early onset of the growing season in spring (Bastos et al., 2020; Lian et al., 2020; Zhang et al., 2021). As illustrated in Figure 1, a soil moisture deficit, that is, the precondition, can result from high evaporation in spring (driven by high temperatures and shortwave radiation) and/or low precipitation. Furthermore, high radiation can favor vegetation growth in spring (when water is not limiting), increasing transpiration. Both effects increase evapotranspiration (ET), ultimately depleting soil moisture. Consequently, spring weather conditions can increase the vulnerability of vegetation to summer drought and heat. To investigate this effect, we ask: does accounting for spring weather conditions improve the prediction of summertime vegetation impacts?

2.2. Case Study

We focus on forests and croplands in the northern mid-latitudes (30°–55°N), where we expect the effect of meteorological drought to be largest due to the close link between vegetation activity and spring onset (Bastos et al., 2020; Buermann et al., 2018; Lian et al., 2020; Zhang et al., 2021). The analysis is carried out separately for croplands and forests as we expect that rainfed croplands are more sensitive to springtime preconditioning effects than forests, which have deeper access to water and are more conservative in their water use over the growing season (Bastos et al., 2014; Flach et al., 2018; Teuling et al., 2010).

2.3. Data

We employ temperature (T), precipitation (P), and shortwave incoming solar radiation (SSRD) from the ERA5 reanalysis data set for the period 1981–2018 (Hersbach et al., 2020). Although ERA5 data should be used with caution for localized extreme events on daily timescales (Jiang et al., 2021; Rivoire et al., 2021),
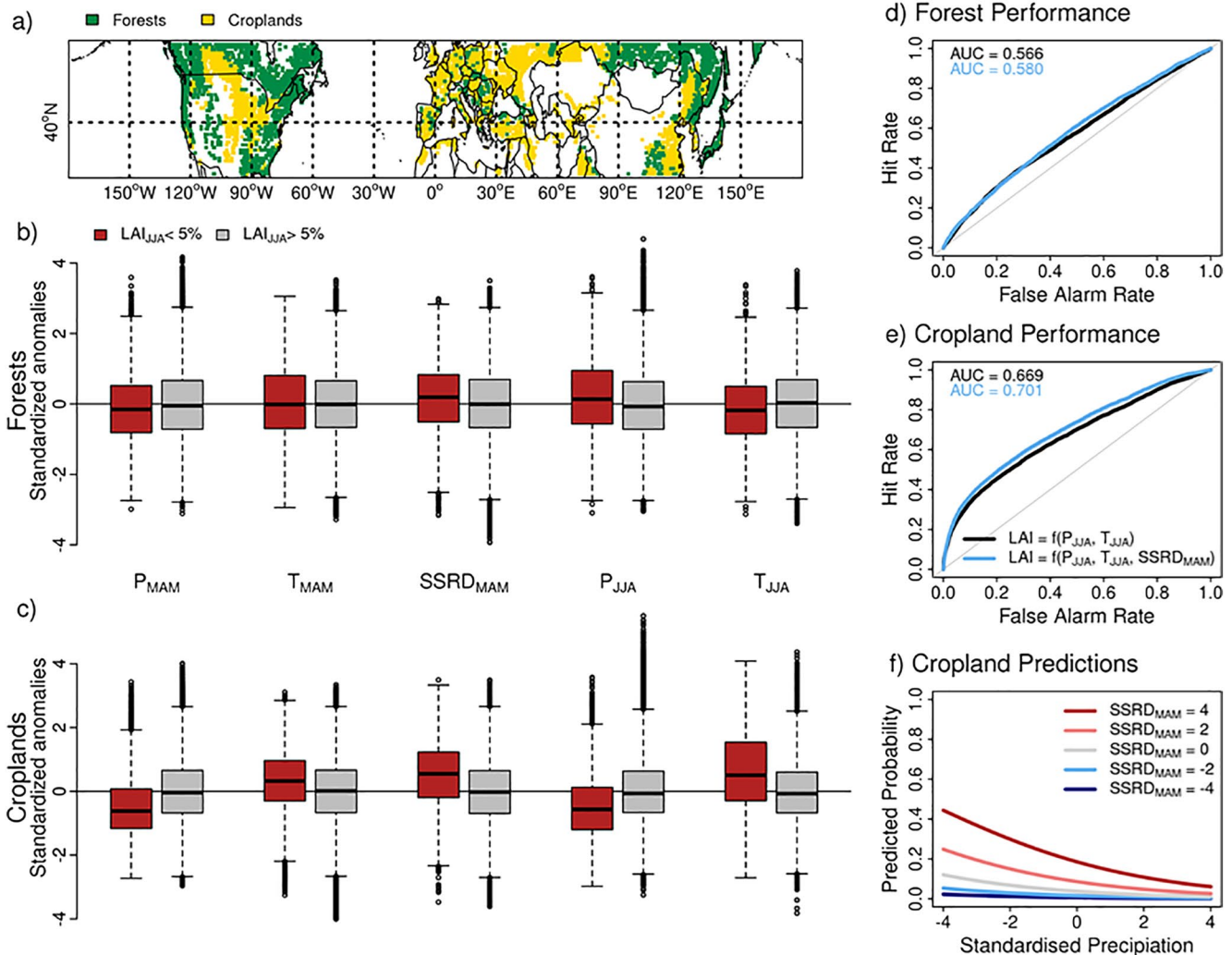
Figure 2. (a) Geographical distribution of forest (green) and cropland (gold) grid cells. For (b) forests and (c) croplands: composites of spring (MAM) and summer (JJA) temperature (T), precipitation (P), and radiation (SSRD) in years with extremely low summer leaf area ($LAI_{JJA} < 5^{th}$ percentile, red) and the remaining years (gray). Boxplots indicate the median (line), interquartile range (box) and 1.5 times the interquartile range (whiskers). Performance of the logistic regression model (based on ROC curves) fitted for (d) forests, and (e) croplands. ROC curves are plotted for two separate models, i.e., the reference model (black) and the model that includes spring radiation $SSRD_{MAM}$ (light blue), along with the corresponding area under the curve (AUC). Note, the larger the AUC, the better the model. The differences in AUC of the two models are statistically significant for croplands (*p*-val < 0.01) and not significant for forests. (f) Predicted probabilities of extremely low (< 5th percentile) summer LAI given specified values of P_{JJA} (*x*-axis) and $SSRD_{MAM}$ (colors), while T_{JJA} is set to its mean value (i.e., $T_{JJA} = 0$).

seasonal/monthly values are more reliable and have been shown to be consistent with observations in space and time (Nogueira, 2020; Tarek et al., 2020). For vegetation data, we employ the Leaf Area Index (LAI) that is derived from Advanced Very High-Resolution Radiometer (AVHRR) satellite data (Claverie et al., 2016). The LAI provides an indication of plant development; high LAI values indicate more growth and healthier plants, and vice versa for low LAI. All variables are first regridded to a 0.5° lat-lon grid via conservative re-mapping (Schulzweida et al., 2006) and then averaged over the spring (MAM: March, April, May) and summer (JJA: June, July, August) seasons. The categorization of grid cells in forest or crop grid cells (Figure 2a) is done using the European Space Agency Land Cover data set (Santoro et al., 2017); see supplementary material for details. We create two datasets for croplands and forest, respectively, by first standardizing all variables per grid cell (subtracting the mean and dividing by the standard deviation) and then pooling grid cells that have the same vegetation type.

2.4. Tools

As a first step, we identify potential drivers of extremely low vegetation activity in summer by building composites of spring/summer meteorological variables corresponding to years with extremely low ($< 5^{th}$ percentile) and not extremely low ($> 5^{th}$ percentile) LAI_{JJA}. Then, we use logistic regression to predict years with extremely low LAI. Specifically, we predict whether summer vegetation is extremely low based on a reference model considering only summertime meteorological conditions as predictors, and test whether the prediction accuracy significantly increases when including springtime meteorological conditions in the model (see Supporting Information S1 for details). We test the performance of the models using Receiver Operating Characteristic (ROC) curves (Mandrekar, 2010; Postance et al., 2018), as well as a summary metric of the ROC known as the Area Under the Curve (AUC). A maximum AUC of 1 indicates a 100% hit rate with no false alarms; the higher the AUC is, the better the model.

2.5. Results and Discussion

In line with Figure 1, extremely low LAI_{JJA} in croplands are associated with precipitation, temperature, and radiation anomalies in both spring and summer (Figure 2c). For forests, these anomalies are much smaller, particularly in spring, and show opposite patterns compared to croplands in summer (Figure 2b).

Using a logistic regression model, we investigate if the prediction of extremely low LAI_{JJA} is improved by adding spring conditions to a reference model that considers only summertime hot and dry conditions (i.e., T_{JJA} and P_{JJA}). For forests, including spring radiation ($SSRD_{MAM}$) does not improve the model's prediction (Figure 2d), while in contrast, a significant improvement (*p-val* < 0.001) is found in croplands (Figure 2e). The fitted coefficients of the logistic regression model also reveal that the meteorological variables have a stronger influence on crops ($SSRD_{MAM}$: 0.44, T_{JJA}: 0.44, P_{JJA}: −0.31) than forests ($SSRD_{MAM}$: 0.17, T_{JJA}: −0.12, P_{JJA}: 0.18). Therefore, hereafter we focus on the effect of spring conditions on cropland only. Note that replacing $SSRD_{MAM}$ with P_{MAM} yields the same performance (whose consequence is discussed later), while adding T_{MAM} does not improve the performance.

For croplands, based on the logistic regression model, we estimate the contribution of $SSRD_{MAM}$ to the probability of a low LAI_{JJA}. For simplicity, probabilities of low LAI_{JJA} are predicted as a function of P_{JJA} and $SSRD_{MAM}$, while T_{JJA} is set to its mean value. The probability of low LAI_{JJA} increases with decreasing P_{JJA} and increasing $SSRD_{MAM}$ (Figure 2f). Hence, cropland impacts are highest when summer with low precipitation follows a spring with high radiation. For instance, the probability of an extremely low summer cropland LAI given a dry summer ($P_{JJA} = -2$) and a normal spring ($SSRD\_MAM = 0$) is 0.1, but increases to 0.3 for $SSRD_{MAM} = 4$. Furthermore, for $T_{JJA} = 2$ and $P_{JJA} = -2$, indicative of a hot and dry summer, this probability increases to 0.5. Overall, the above indicates that spring weather conditions favoring low soil moisture can affect the vulnerability of vegetation to a hot and dry summer over croplands.

In our model, replacing $SSRD_{MAM}$ with P_{MAM} yields the same performance, indicating that soil moisture deficits can be modulated by either or both high radiation and low precipitation (which often coincide) through the two mechanisms illustrated in Figure 1. Here, it is not possible to disentangle the relative contributions of the two mechanisms, though the depletion of soil moisture in spring via crop growth is supported by the fact that dry soils in summer are often preceded by increased springtime vegetation growth resulting from an early spring onset (Lian et al., 2020) that would allow for high radiation throughout the spring season. The relative difference in model improvements between forests and crops (Figures 2d and 2e) due to the inclusion of spring conditions, may suggest a role of vegetation type in developing a soil moisture deficit. However, due to their deep root systems that provide greater access to moisture, forests are generally more vulnerable to consecutive than single drought events (Anderegg et al., 2020), therefore the results may simply highlight that forests are less vulnerable during single droughts than crops. In future analyses, it would be interesting to take into account the memory held in an ecosystem of previous drought events in order to understand its influence on the impact from the precondition and hazards, which remains a challenging undertaking (e.g., Chauhan & Ghosh, 2020). Furthermore, here we combined data from different locations which has the advantage of increasing the sample size and obtaining more robust statistics, but

the disadvantage of not allowing for disentangling spatial variations in the vegetation responses to weather conditions. As a result, the differences found between cropland and forest may arise from the fact that in our data set there are more cropland than forest grid cells below 40°N, that is, regions where evapotranspiration is not limited by energy constraints (Zscheischler et al., 2015). Removing these grid cells reduces the model improvement achieved by adding spring radiation, suggesting that its influence is not uniform across the studied domain.

Process-based vegetation models, simulating the response of vegetation to atmospheric variables based on underlying physiological processes, could allow for disentangling the effects of a precondition in follow-up studies. These models provide an advantage over statistical models as they would allow for disentangling the direct role of vegetation in exacerbating springtime soil moisture deficits using counterfactual simulations (Bastos et al., 2020). Importantly, process-based vegetation models are expensive to run and require carefully designed spin-up and simulation protocols as well as multi-model ensembles to properly account for uncertainties. Our results highlight the need of including vegetation dynamics in simulations of future climate in order to account for the influence of the discussed vegetation feedbacks to projected longer and warmer growing seasons in spring (Lian et al., 2020).

2.6. Link to Other Preconditioned Events

The approach outlined here can be used as a guideline to assess other preconditioned events. Each event type will require its own specific considerations (e.g., definition of hazards, identification of potential preconditions) but the structure of the conceptual model and its components will be similar. For instance, Gudmundsson et al. (2014) used logistic regression to predict increased wildfire activity after a meteorological drought. In fact, wildfires occurrences can be enhanced by previous-year surface moisture conditions (Forkel et al., 2012). In another example, either or both soil moisture and extensive snow cover can enhance river floods triggered by storm-driven precipitation extremes (Berghuijs et al., 2016, 2019).

3. Multivariate Event: Future Changes in Compound Coastal Flooding

### 3.1. Introduction and Research Question

A typical example of multivariate compound events is compound coastal flooding (CF), which occurs when high sea levels obstruct the gravity-driven flow of pluvial/fluvial water into the ocean (Couasnon et al., 2020; Eilander et al., 2020; Ganguli et al., 2020; Wahl et al., 2015). Recent large-scale studies indicate that CF drivers such as precipitation, river discharge, or sea-level extremes will change in a warmer climate (Bevacqua, Vousdoukas, Zappa, et al., 2020; Moftakhari et al., 2017; Winsemius et al., 2016), which may have a significant impact on flooding at the local scale. In this context, we ask: how will climate change affect the CF hazard at the local scale?

3.2. Case Study

The above question is considered for the Swan River estuary (catchment area 124,000 km^2), which flows through the densely populated city of Perth, in the state of Western Australia, Australia. Here we focus on the climate-driven component of the flooding risk, however note that urbanization is important to ultimately determine flooding impacts.

3.3. Data

We use observed daily maxima obtained from hourly or sub-hourly time series (1990–2015) of: water levels at the Barrack station near Perth City (about 20 km inland and influenced by compound effects), upstream river discharge at the Walyunga stream gauge, and sea water levels at the coast at Fremantle. We focus on the period of May-August, when both water levels and discharge are the highest. Prior to extracting daily maxima, the sea-level data is decomposed into the astronomical tide and non-tidal residuals (i.e., mainly storm surge driven by meteorological fluctuations). To characterize the underlying process leading to CF, we also use daily accumulated precipitation and mean sea-level pressure fields from the ERA5 reanalysis
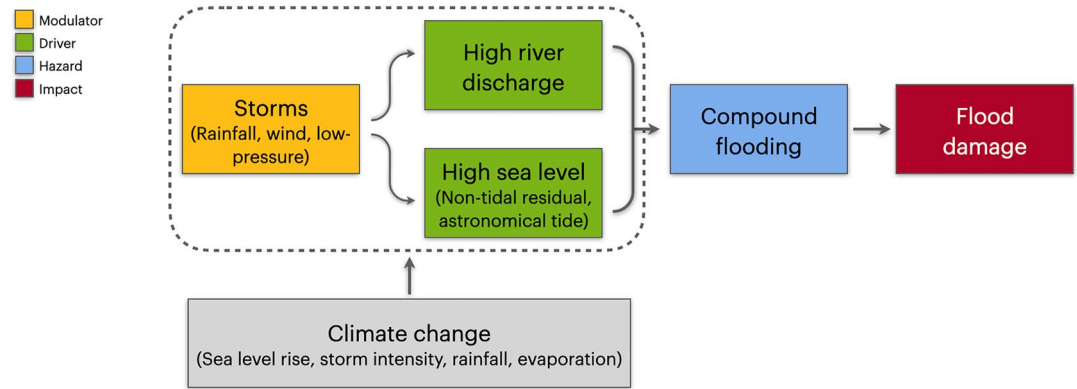
Figure 3. Physical elements of compound coastal flooding damages in Perth, Australia, caused by the extreme compound water level due to interacting flood drivers. Weather systems such as storms modulate the intensity of the drivers via processes such as winds, pushing the oceanic water toward the coast, and rainfall. Note that rainfall from more than one storm and also evaporation can modulate river discharge. Climate change can affect compound flooding via sea-level rise, changes in storm intensity and duration, associated rainfall, and evaporation. Arrows indicate causal links.

data set (Hersbach et al., 2020). For future projections, we discuss plausible changes in the compound flooding drivers that are extracted from the available literature (see references within the text).

3.4. Tools

We use a multivariate non-linear regression model (James et al., 2013) to quantify the present-day influence of the river discharge (Q), astronomical tide (T_{astr}), and non-tidal residuals (S) on the *compound water level* at the Barrack station (H), that is,

$$H = a_1 \ Q + a_2 \ (T_{astr} + S) + a_3 \ Q \ (T_{astr} + S) + \epsilon(c, \sigma), \tag{1}$$

where a_i are the regression coefficient and $\epsilon(c, \sigma)$ is the error term. Composite maps (i.e., average weather conditions), and lagged correlations are used to investigate CF drivers (Klerk et al., 2015; Ward et al., 2018).

3.5. Results and Discussion

To assess CF changes in a warmer climate, it is important to first understand the processes shaping present-day flooding (Figure 3). The multivariate regression model (Equation 1; $R^2 = 0.997$) indicates that the water levels in Barrack are compounded by sea levels and river discharges, however mainly influenced by the sea levels (gray isolines in Figure 4b). (Note that all parameters in Equation 1 are significantly different from zero and that, based on the Akaike information criterion (AIC), the two models considering an individual predictor, that is, Q only or (Tastr + S) only, have a lower quality than the model in Equation 1.) More upstream in the estuary the sea's influence diminishes (Bilskie & Hagen, 2018; Gori et al., 2020), hence we expect more pronounced compound effects, that is, discharge and sea levels to have a similar impact on the water levels (orange isolines in Figure 4b) (Eliot, 2012; Helaire et al., 2020; Wu et al., 2021).

Since water levels at Barrack are largely driven by sea levels, extremes (here, annual maxima) in both compound water levels and non-tidal residuals are driven by similar atmospheric configurations (Figures 5a and 5b). Non-tidal residual extremes (annual maxima) are favored by an elongated region of low atmospheric pressure, that is, stormy weather, via winds pushing toward the coast and low barometric pressure effect (Bevacqua et al., 2017). Such atmospheric configuration is associated with wet conditions on the river catchment, however, in line with the time needed by the accumulated rainfall to reach the discharge gauge through the large catchment (Figure 5c) (Bevacqua, Vousdoukas, Shepherd, & Vrac, 2020; Hendry et al., 2019), high river discharges at the outlet tend to occur 3–4 days after high non-tidal residuals (Figure 5d). This lag time can vary per event and is dependent not only on catchment size, but also on effective flow path, vegetation cover, and land use.
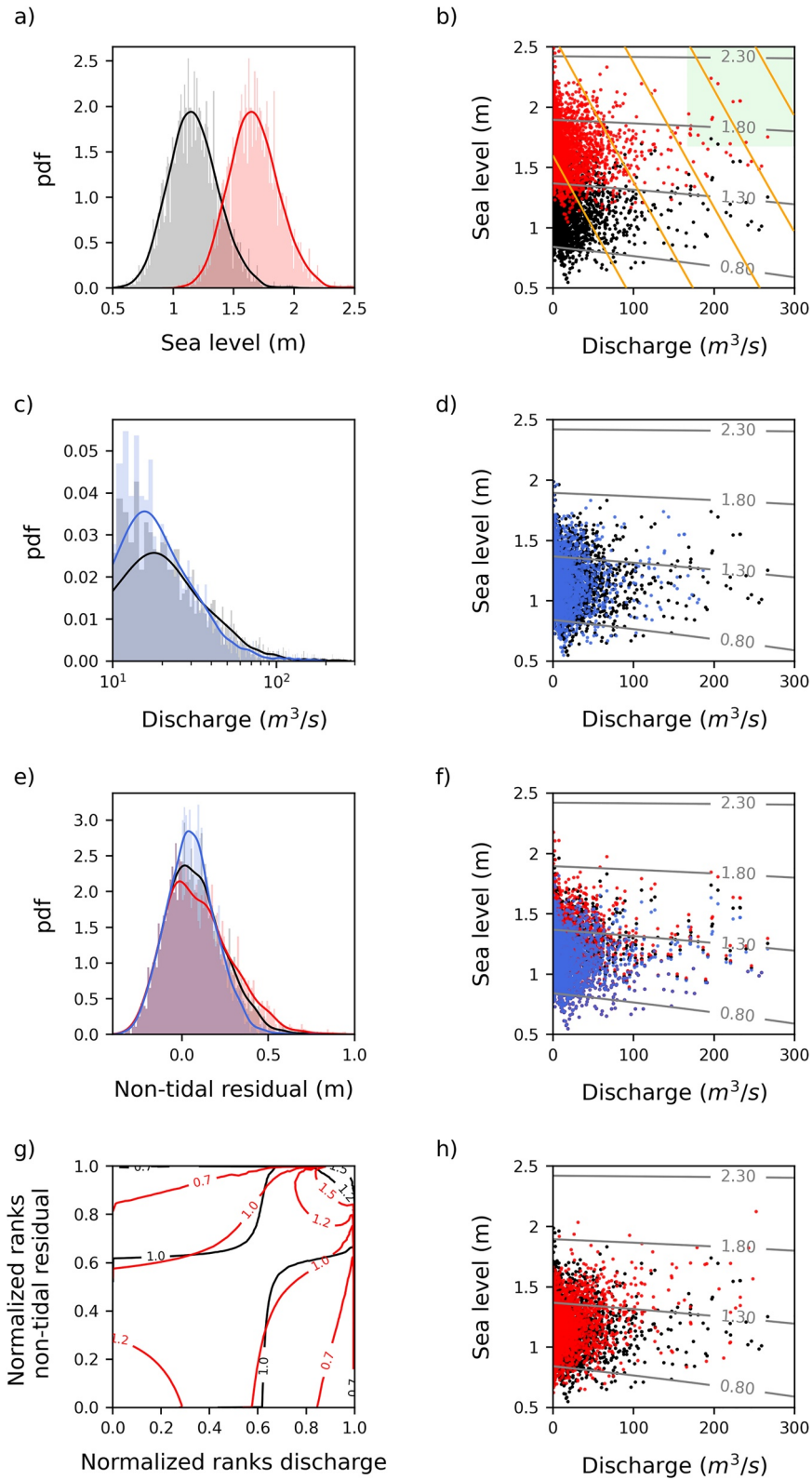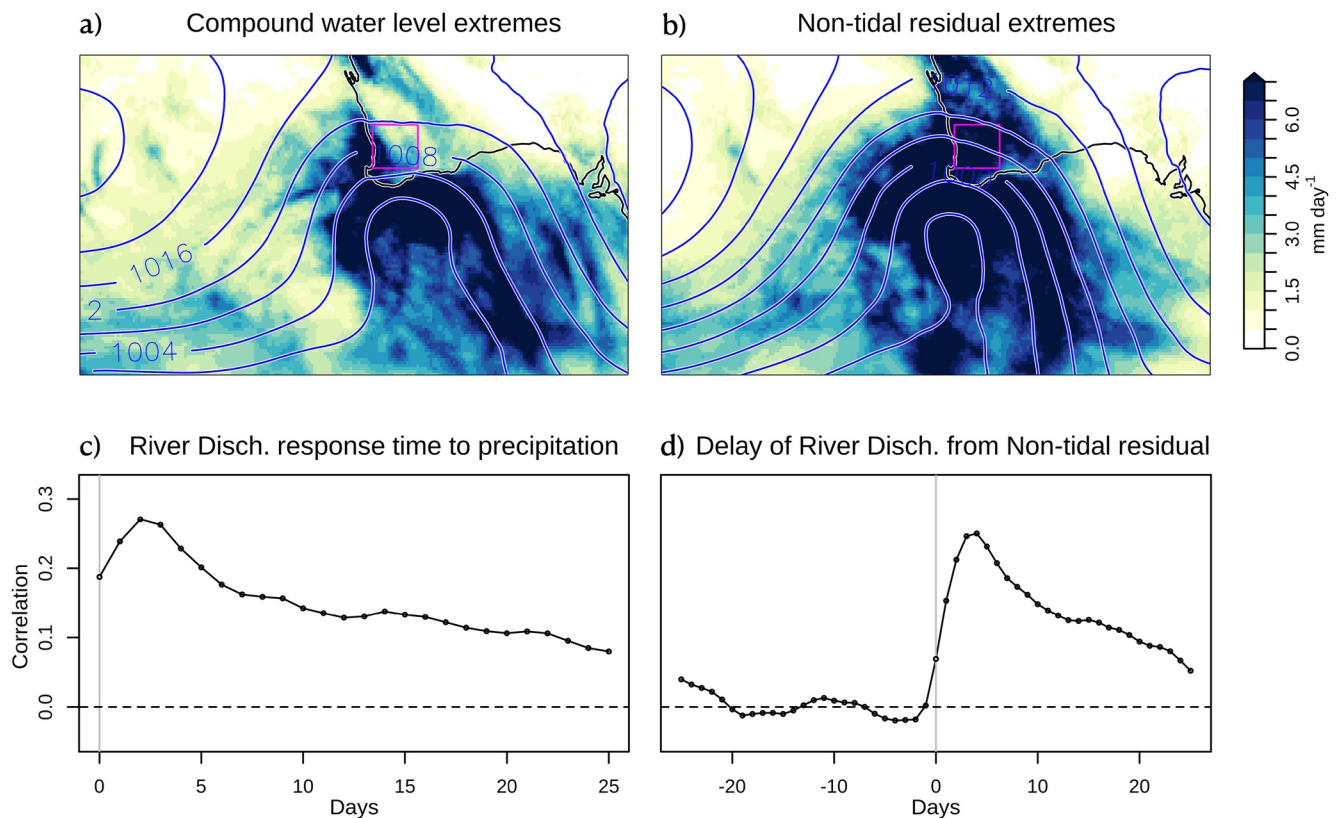
Figure 4.

Figure 5. Composite maps of sea-level pressure (hPa; blue contours) and daily accumulated precipitation (shading) during days characterized by the top eight (out of 16) annual maxima of (a) compound water level in Barrack and (b) non-tidal residuals at the coast. The rectangle in magenta indicates the outlet of the river catchment and estuary. (c) Pearson correlation between the daily discharge on day t and the precipitation aggregated on the river catchment on day t-N (on the x-axis), where the lag maximizing the correlation provides a first-order estimate of the time needed by the precipitation to reach the discharge gauge. (d) Lagged correlation similar to (c), that is, between daily river discharge and non-tidal residual on day t-N indicating that a higher river discharge tends to follow a higher non-tidal residual with a delay of about 3–4 days.

By the end of the century, changes in river discharge, sea levels, and their interplay can largely affect flooding dynamics. However, flooding projections remain unclear due to uncertainties in anthropogenic forcing scenarios, internal climate variability, and climate model differences. While we detected rare concurrent river discharge and sea-level extremes in the present, sea-level rise could increase CF risk (Moftakhari et al., 2017). For example, under a plausible sea-level rise of 0.5 m (Figure 4a), which is in line with Hope et al. (2015) and Vousdoukas et al. (2018), present-day river discharge extremes and mild sea levels would become concurrent extremes (dashed area in Figure 4b) (Bevacqua et al., 2019). However, climate projections point toward a reduction in discharge extremes by 20%–50% (Figure 4c) (in line with Evans & Schreider, 2002; Hirabayashi et al., 2013; Swan River Trust, 2007), which could decrease CF risk (Figure 4d). Changes in storminess are uncertain and could lead to an increase or decrease (Figure 4e) in non-tidal residuals (Hope et al., 2015; Vousdoukas et al., 2018) and consequently in CF risk (Figure 4f). Changes in the dependence between non-tidal residual and river discharge (Figure 4g) may affect flooding as well

Figure 4. (a) Observed (black) and a plausible future (red) distribution of sea levels, where mean sea level increases by 0.5 m. (b) Corresponding observed and plausible future pairs of sea levels and discharge Q, where the future sea level distribution is taken from (a) and Q distribution is the observed. The other rows are the same as in (a and b), but consider: (c and d) a plausible future decrease (blue) in Q by 30%; (e and f) plausible future increase (red) and decrease (blue) in positive non-tidal residuals, that is, S, by 20%; (g and h) a potential future increase in the dependence between Q and S (g and h). In (g), black isolines represent the parametric copula density derived from data (a survival Clayton copula, selected based on the AIC among a pool of copulas available in the VineCopula package [Schepsmeier et al., 2016]); red isolines show a potential future copula with higher dependencies (i.e., copula parameters were modified increasing Kendall's tau from 0.04 to 0.3 and the upper tail dependence coefficient from 0.0001 to 0.15). Gray isolines in the right-hand panels show the average compound water level in Barrack predicted by the multilinear regression model. In (b), orange isolines show how the compound water level may be influenced by sea level and Q in a hypothetical location upstream (water levels increasing from bottom-left to top-right); and the green dashed area indicates concurring sea level and Q extremes (> observed 99th percentiles). Plausible future changes in flood drivers are based on literature (see main text).

(Figure 4h), however these changes remain uncertain and understudied (Bevacqua, Vousdoukas, Zappa, et al., 2020). We move to discuss different tools/approaches for assessing the effect of the changes above on local CF.

Statistical models for estimating compound water levels, such as the multivariate regression model employed here (Bermúdez et al., 2019; Santos et al., 2021), are often derived from (short) observational records. This can affect model accuracy under climate change, when information needs to be extrapolated far beyond the observed range. High-resolution *hydrodynamic models*, which include the non-linear interaction between hydraulic processes, topography, and human interventions (Kumbier et al., 2018; Mohanty et al., 2020; Wu et al., 2021), can provide a valid alternative for a thorough CF analysis. Hydrodynamic modeling can provide a detailed spatial mapping of water levels in the estuary, for example, it can be used to quantify the relative contribution of flood drivers (Mohanty et al., 2020) and the spatial variability of socio-economic impacts of flooding depending on the level of urbanization within the estuary, which can influence runoff characteristics (Olbert et al., 2017; Sebastian et al., 2019). Furthermore, hydrodynamic simulations can highlight peculiar features of the hydrological system (Khojasteh et al., 2021), for example, directly accounting for a potential shift in the area affected by compound effects from future sea-level rise (Bilskie & Hagen, 2018; Helaire et al., 2020). *Probabilistic approaches* can be applied to assess future flood return levels using simulated multi-year water-level time-series via high-resolution hydrodynamic modeling forced by an ensemble of climate models. However, running these simulations is computationally expensive, though approaches to circumvent this have been suggested (Parker et al., 2019; Sopelana et al., 2018; Wu et al., 2021). Nevertheless, applying a probabilistic approach for local future risk assessment remains challenging since no probability is attached to anthropogenic forcing scenarios. Notably, even focusing on a given anthropogenic forcing scenario, multimodel ensembles cannot be interpreted probabilistically (Zappa & Shepherd, 2017).

In this context, we suggest employing hydrodynamic models to study *event-based storylines* which explore in detail low-likelihood, high-impact future plausible events, with an emphasis on plausibility rather than probability (Hazeleger et al., 2015; Shepherd, 2019). Event-based storylines can be built based on expert knowledge, major past floods (Helaire et al., 2020; Khanam et al., 2021), or near-misses (Woo, 2021). One could investigate: what would be the societal impact of past fluvial flooding combined with the projected sea-level rise? Which consequences would a past storm have under a projected scenario with sea-level rise, high astronomical tide and reduced streamflow? What if a sequence of storms, the first causing high river discharge at the outlet and the last a concurring storm surge, had to hit Perth? Initial-condition large ensemble simulations and seasonal-hindcasts can help identify plausible threatening combinations of drivers that could lead to unseen extreme impacts (Thompson et al., 2017; Van der Wiel et al., 2021). Storylines fit well within common practices in disaster risk management, which consider event-based scenarios for emergency preparedness (Sillmann et al., 2021), and also allow for interaction with local stakeholders to evaluate the effectiveness of selected measures, for example, dam installations and use.

3.6. Links to Other Multivariate Compound Events

The methods above can be used to study other multivariate compound events. Composite maps can help to identify the atmospheric drivers of, for example, wildfires, crop failures, tree mortality, which are often associated with hot and dry conditions (Hoerling et al., 2013; Hao et al., 2019; Zscheischler et al., 2020). Combined with large ensemble climate model simulations (Deser et al., 2020), composites can help to identify drivers of, for example, extremely low renewable energy production (Van der Wiel, Stoop, et al., 2019). The knowledge acquired from composites can, for example, also allow for assessing how extreme events conditional to identified impact-driving weather patterns may evolve in the future (Jézéquel et al., 2020). Regression and more sophisticated models can help studying landslides (from precipitation, evaporation, and snowmelt), avalanche risk (enhanced by wet and warm conditions), and impacts from concurrent wind and precipitation extremes (Martius et al., 2016). In general, event-based storylines can provide practical information targeted to users' needs, for example, for planning adaptation to plausible extreme events.
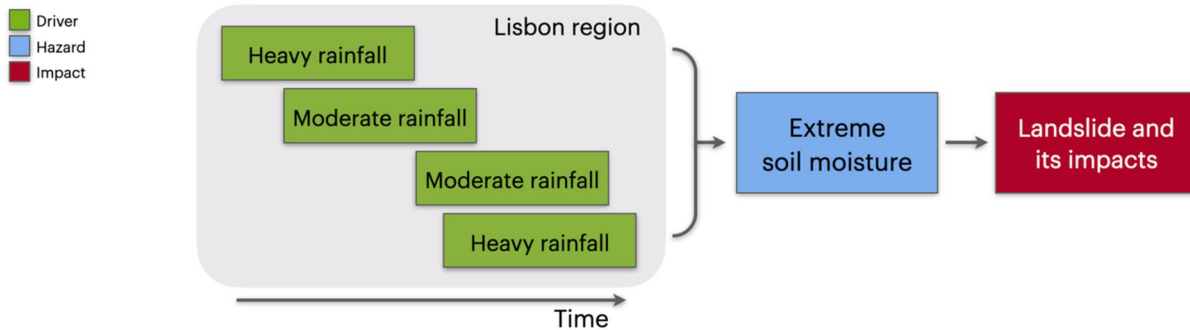
Figure 6. Physical elements of landslides and associated impacts in Portugal arising from extreme soil moisture, which is driven by clusters of moderate to extreme rainfall events. Arrows indicate causal links. Note that evaporation also influences soil moisture, but such a relationship is not represented here given the focus of the research question on precipitation clustering.

4. Temporally Compounding Event: Precipitation Clustering Favors Landslide Occurrences

4.1. Introduction and Research Question

Landslides are a localized natural hazard that can result in fatalities and severe socio-economic losses (Froude & Petley, 2018; Petley, 2012). From a geological perspective, landslides are classified as shallow or deep based on the depth of the soil sliding surface. For both landslide types, accumulated precipitation that saturates the soil, therefore reducing its shear strength, is one of the most important drivers (Figure 6) (Guzzetti et al., 2007). Shallow landslides are typically triggered by one or several intense precipitation events falling within 1–15 days before the landslide, while deep landslides generally occur as a result of rainfall accumulated over weeks to about three months (Zêzere et al., 2015). Previous studies have quantified the critical accumulated precipitation amounts that can trigger landslides (Brunetti et al., 2010; Guzzetti et al., 2007; Peruccacci et al., 2017; Zêzere et al., 2015). Given that accumulated precipitation extremes are often caused by clusters of precipitation events from multiple storms (Bevacqua, Zappa, & Shepherd, 2020; Dacre & Pinto, 2020; Priestley et al., 2017) sometimes in association with individual atmospheric rivers (Hénin et al., 2021; Ramos et al., 2015), here we investigate whether a clear relationship between precipitation clustering and landslides can be identified. Specifically, we ask: are deep- and/or shallow-landslides preceded by temporal clustering of moderate to extreme rainfall events?

4.2. Case Study

We focus on the region north of Lisbon (Portugal), which has a high landslide risk (de Brum Ferreira & Zêzere, 1997; Pereira et al., 2020). The region is part of the Western Meso-Cenozoic borderland, which has the highest number of disastrous landslides in Portugal (about 10 cases per 10^3 km^2 during 1865–2010) (Zêzere et al., 2014).

4.3. Data

We analyze the period 1956–2008, for which 23 landslides events were recorded in the data set (Zêzere et al., 2015). A landslide event is identified when a minimum of five individual landslides occurred on natural slopes on a given date (Zêzere & Trigo, 2011). Following Zêzere and Trigo (2011), a landslide event was classified as shallow if more than 50% of the landslide area has a slip surface depth ≤1.5 m and as deep otherwise. For precipitation, we employ the daily high-resolution (0.2° lat-lon grid) IBERIA02 data set (Belo-Pereira et al., 2011; Ramos et al., 2014) selecting a single grid-point, the nearest to the location of the landslides.

4.4. Tools

In a four-step procedure, we quantify whether landslides are systematically preceded (within a certain temporal window before the landslides) by a cluster of moderate to extreme precipitation events.

1. We identified the occurrence of precipitation events, here daily precipitation amounts above 9.25 mm (i.e., the year-round 85th percentile of daily amounts; such threshold allow for considering moderate to extreme events, potentially relevant for landslides). To disentangle occurrences arising from different weather systems, we filtered high-frequency clustered events, that is, groups of daily events less than 3 days apart were categorized as a unique precipitation event (dated as the earliest event in the group), which satisfy the *iid* condition for frequency analysis (Barton et al., 2016; Ferro & Segers, 2003).
2. We quantified the typical number of precipitation events occurring in any given temporal window W_t, noticing that the number of events N_{W_t} within W_t is Binomially distributed ($B(W_t, p)$; p is the probability of a precipitation event on any given day).
3. For a window W_t before any given landslide of interest, we identified a precipitation cluster when the number of precipitation events N_{W_t} was above the 95th percentile of the Binomial distribution (at 5% significance level). To prevent making strong assumptions on the width of the window W_t, we sequentially looked for clustered events in all of the 87 backward windows W_t starting on the day of the landslide and ending 4–90 days before the landslide (a correction for multiple tests was applied, see Supporting Information S1).
4. After repeating the procedure above for each landslide, we quantified the fraction (%) of landslides that were preceded by precipitation clustering (we employed bootstrap to assess whether such a fraction is significantly higher than expected under independence between landslides and precipitation clustering).

See Supporting Information S1 for details on the methods.

4.5. Results and Discussion

In the Lisbon region, all of the 23 registered landslides occurred during the period November-March, of which 11 were classified as deep and 12 as shallow (in blue and red in Figure 7a, respectively). This period of the year is characterized by the highest frequency of 3-day accumulated precipitation extremes (Bevacqua, Vousdoukas, Zappa, et al., 2020), indicating precipitation's relevant role for landslide occurrences. In addition, here we demonstrate that most (deep) landslides were preceded by clustering of precipitation events.

Figure 7a shows whether clusters of precipitation events were detected in the windows [-n, 0] days preceding any landslide. For example, for the shallow landslide in 1983, the brown rectangle 23 days before the landslide indicates that an anomalously high number of precipitation events occurred in the window [-23, 0] days before the landslide. Altogether, we detected precipitation clustering (at least one marked rectangle) before 83% (19/23) of landslides. Notably, this fraction is larger than 30%, which is the 95th percentile of the value expected under no association between landslides and precipitation. However, while all deep landslides (11/11%, 100%) were associated with clustered precipitation events, the association is weaker for shallow landslides (8/12%, 67%). This difference indicates that multiple consecutive precipitation events are a crucial driver of deep-landslides, while—in line with previous studies (e.g., Zêzere et al., 2015)—shallow-landslides can also be triggered by single precipitation events.

Given the different geological nature of deep and shallow landslides (Zêzere et al., 2015), we investigate whether clustered precipitation events preceding deep and shallow landslides have different temporal characteristics. That is, for deep- and shallow-landslide events separately, we quantify the fraction of events that are preceded by precipitation clustering over different time windows. In line with the above, the results indicate that precipitation clustering may favor both landslide types. Still, major differences between the two landslide types are identified (Figure 7b). In fact, about 70%–83% of deep landslides are significantly preceded by precipitation clustering over long temporal windows of 23–90 days, in line with multiple precipitation events rising groundwater level of deep soil and rock layers (e.g., Iverson, 2000). In contrast, only about 7%–9% of shallow landslides are significantly preceded by clustered precipitation events, which occur 4–25 days before the landslides.
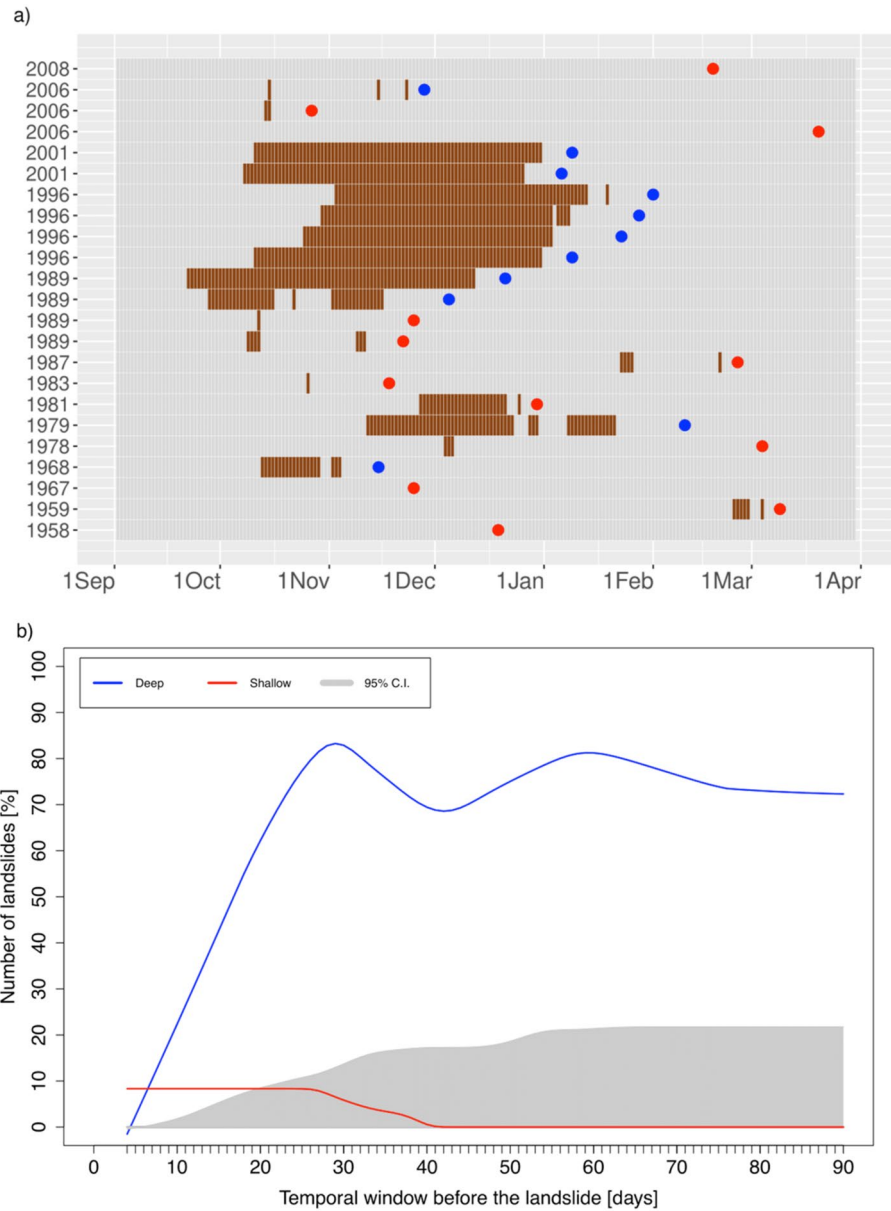
Figure 7. (a) Temporal clustering of moderate to extreme rainfall events before the 23 studied landslide events. Blue dots indicate the deep landslides, red dots the shallow landslides. The brown bar indicates the start date of the temporal window (W_t) ending the day before the landslide event, when the temporal clustering of rainfall was detected. Note that August is not shown because no clustering was detected in windows starting within this month. (b) Percentage of deep (blue) and shallow (red) landslides preceded by precipitation clustering in each temporal window between 4 and 90 days. The gray shading illustrates the 95% confidence interval (i.e., the 95th percentile) of the number of landslides preceded by precipitation clustering under the assumption of no association between precipitation clustering and landslide events (obtained via shuffling the data, see Supporting Information S1). Counts are first obtained for each temporal window, then curves are obtained via a Locally Weighted Scatterplot Smoothing (LOWESS) with a smoothing parameter equal to 1/3.

Precipitation clustering are associated with the passage of multiple storms and intensified westerly flow, leading to continuous pulses of moist air masses approaching the Iberian Peninsula (Hénin et al., 2021). Our results indicate a causal relationship between precipitation clustering and landslides, especially for deep landslides, which is in line with physical understanding (Figure 6). In line with previous studies, shallow-landslides can be caused by individual precipitation events exceeding critical thresholds (Gariano et al., 2015; Guzzetti et al., 2007). Notably, given that the classification of deep and shallow landslides is

based on geological features, the contrasting results found for the two landslide types are directly attributable to differences in the meteorological processes causing the landslides. Here, we focused on low-frequency precipitation clustering, hence we do not exclude that also high-frequency clustering, for example, from multiple convective precipitation events occurring within a few (< 3) days, is a relevant driver of shallow-landslides. Further analyses based on a combination of physically based modeling with analyses of meteorological conditions and counterfactual experiments could allow investigating more in-depth questions related to the cause-effect relations of landslides.

4.6. Link to Other Temporally Compounding Events

An approach similar to the one developed here could be employed to investigate the relevance of event clustering for other types of natural hazards or impacts. For example, it could allow for identifying areas where temporal clustering of precipitation extreme events causes lake and river flooding, as well as high accumulated precipitation extremes (Barton et al., 2016; Bevacqua, Zappa, & Shepherd, 2020). Similarly, it could be possible to investigate whether sequential multi-year droughts have an impact on, e.g., forests (Anderegg et al., 2020) and how losses to the insurance industry are affected by consecutive storms (Priestley et al., 2018). It would also be possible to consider clustering of multiple hazard types, e.g., to study the negative effects of consecutive precipitation and temperature extremes on societies (Baldwin et al., 2019; Matthews et al., 2019; Ruiter et al., 2020; Zhang & Villarini, 2020).

5. Spatially Compounding Event: Synchronous Wheat Failure Across European Countries

5.1. Introduction and Research Question

Synchronous crop failures across multiple countries can pose a high risk to international food security and supply chains (Anderson et al., 2019; Gaupp et al., 2019) as exemplified by the European crop failure in 2018 (Beillouin et al., 2020; Toreti et al., 2019). Therefore, for society to be resilient to large-scale crop failures, it is important to reliably assess the probability that crop failure can be caused by spatially compounding events and also understand the drivers of behind these failure events. In this context, we ask: does the interplay between crop failures in different European countries affect aggregated continental crop yields? What are the climate drivers of such continental crop failures?

5.2. Case Study

We analyze the concurrent failure of wintertime wheat across Europe (wintertime wheat is planted at the beginning of the winter and typically harvested in summer around July). We mainly focus on France and Germany (Figure 8), which are the two largest European wheat producers and therefore strongly influence continental food security (FAOSTAT, 2021).

5.3. Data

We use large-ensemble simulations that consist of 1600 growing seasons and associated annual wintertime wheat yields from Vogel et al. (2021). Wheat yields were simulated with the APSIM-Wheat model (version 7.10) (Zheng et al., 2014) driven by meteorological data from the EC-Earth global climate model (Hazeleger et al., 2010; Van der Wiel, Wanders, et al., 2019) under present-day (2011–2015) climate conditions. We consider yields aggregated at the country level (Ribeiro et al., 2021), at this country scale the simulated annual wintertime yields compare well with observed yields (Vogel et al., 2021). To investigate drivers of crop failure, we consider mean monthly precipitation, vapor pressure deficit, and maximum temperature fields (Ray et al., 2015).

5.4. Tools

To quantify the effect of the dependence between yields of individual countries, we compare continent-wide aggregated yields from the original data set with those obtained after randomly shuffling annual yields in all
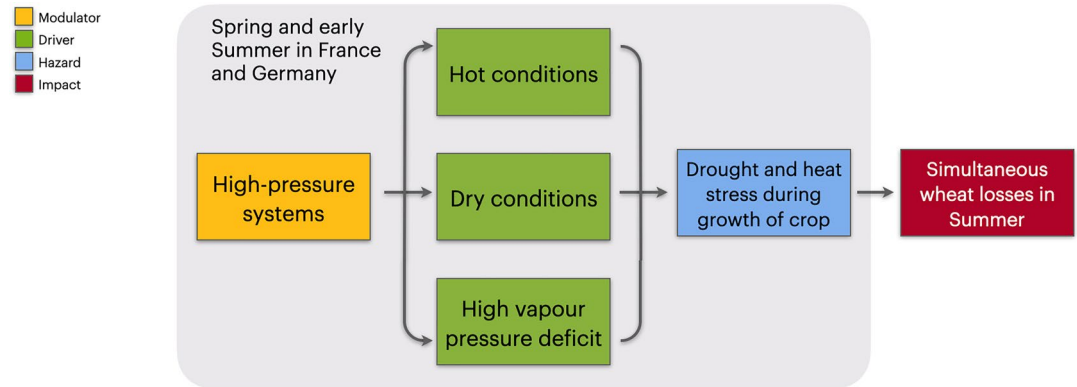
Figure 8. Physical elements of spatially compounding, that is, simultaneous, winter-wheat losses in France and Germany caused by hazardous drought and heat stress during a key period of the growing season (spring and early summer, gray box). The drivers of the hazard, here high temperature, dry conditions, and high vapor pressure deficit, are favored by modulators such as high-pressure systems. Arrows indicate causal links.

countries in time. We assess the relationship between crop yields in France and Germany through correlations and rates of co-occurring extremes. We estimate the probability of the total loss in a year exceeding a given loss amount via Aggregate Exceedance Probability (AEP) curves, which are standard insurance sector plots (Hillier et al., 2015; Hillier & Dixon, 2020; Mitchell-Wallace et al., 2017). To identify meteorological anomalies associated with crop failures, we compare composites (i.e., averages) of both meteorological time series and spatial fields during years with extremely low and normal yield (e.g., Vogel et al., 2021).

5.5. Results and Discussion

At the European scale, the spatial correlation of wheat yields between countries strongly increases the likelihood of years characterized by high and low extreme aggregated yields, compared to the case where national yields are independent (Figure 9a). Accordingly, the wheat production of the two leading European producers, that is, France and Germany, show a positive dependence ($\rho_{Pearson} \sim 0.5$; p-val $\ll 0.01$). Such a relationship also appears for the largest crop failures of the two countries, which tend to co-occur about four times more often than expected under independence (binomial test, p-val < 0.01, Figure 9b). Notably, the dependencies described above can influence European food security. This is illustrated by the AEP curve, indicating that aggregated yield losses of France and Germany with a return period larger than 10-year are about 20% larger than expected under independence (Figure 9c; note that the contribution of the two countries to the aggregated yield differ by only ~10%).

Given the dependence of European wheat yield on Germany and France, we aim to identify the physical processes (Figure 8) associated with concurrent crop failure in both countries. Figure 10 shows that seasons resulting in the lowest 5% aggregated crop yields of Germany and France ("bad" seasons) are associated with high maximum temperature, low precipitation, and high vapor pressure deficit during the growing season in May-July (Figures 10a, 10c, and 10e). We note that during this growing stage, when the vegetation is photosynthetically most active, crops' health is particularly susceptible to the effects of compound warm and dry conditions, inducing vegetation stress that limits the quantity and quality of the harvests (COGECA, 2003; Ribeiro et al., 2020; Vogel et al., 2021). Finally, the composites show that during May-July, bad seasons are characterized by spatially homogeneous anomalies in the weather conditions across Germany and France (Figures 10b, 10d, and 10f), indicating that large-scale weather patterns, such as high-pressure systems, favor aggregated crop failures.

The above highlights that both preconditioning effects during May-July and multivariate contributions from different drivers shape the spatially compounding European wheat failures (in line with the results of Section 2). Preconditioning effects have also been identified as a key driver of the record-breaking 2016 crop failure in France (Ben-Ari et al., 2018).
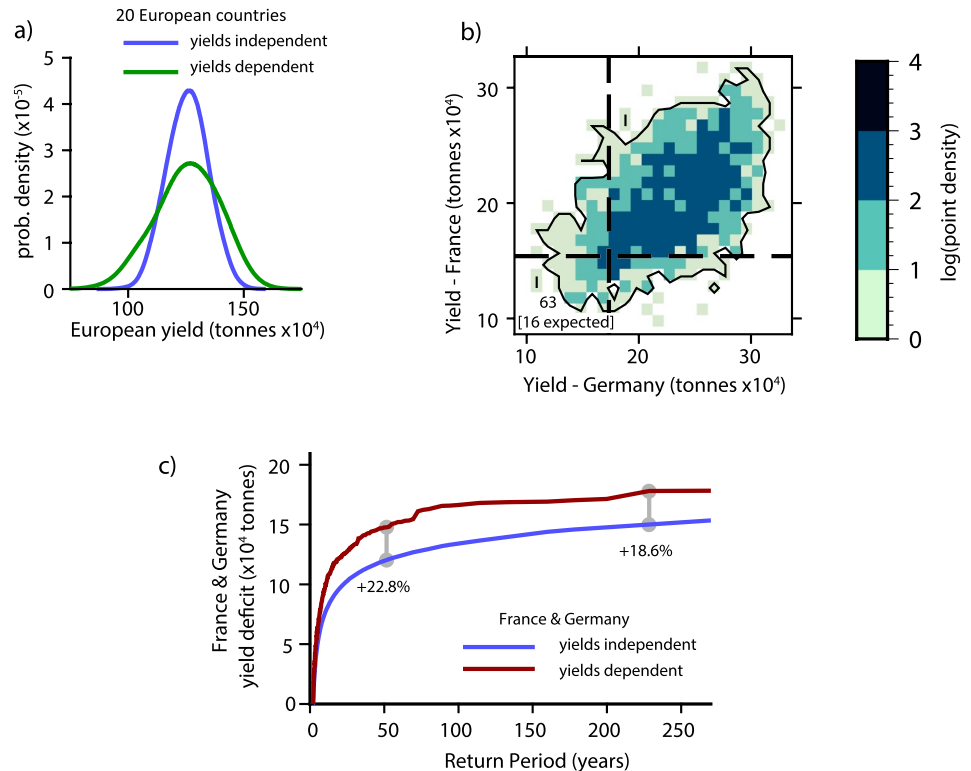
Figure 9. (a) Probability density function (pdf) of the simulated aggregated wheat yield of 20 European countries (blue), against the same obtained computing the aggregated wheat yield after removing the inter-country wheat yield dependencies (green). (b) Bivariate pdf of crop yield of France and Germany. Dashed lines show the empirical 10th percentile for each country. We detect 63 co-occurring extremes, which is about four times larger than 16, that is, the values expected under independence ($0.1^2 \cdot 1600$, where 1600 are the number of simulated seasons). (c) Aggregate Exceedance Probability (AEP) plot of the deficit (i.e., level below mean) of simulated aggregated crop yield of France and Germany (red), and when assuming inter-country independence (blue); labeled at selected return periods. All differences between simulated and independent cases are statistically significant (p-val < 0.01). One hundred permutations and a t-test were used to compute p-values in (c).

5.6. Link to Other Spatially Compounding Events

Spatially compounding events can challenge the ability of (re-)insurance companies and governments to respond to emergencies (Falco et al., 2014; Hillier et al., 2020; Jongman, 2018; Raymond et al., 2020). An increasing need for adapting to climate change in many sectors such as agriculture, energy, industry, buildings, and transport (Hoegh-Guldberg et al., 2018), further highlights the relevance of studying these events. Our approach can be extended to investigate crop yields at the global scale and to analyze other major crop types such as maize and soy (Mehrabi & Ramankutty, 2019). For example, composites would allow for identifying typical atmospheric configurations associated with concurrent low agricultural production across the main "breadbasket" regions worldwide (Gaupp et al., 2019; Kornhuber et al., 2019). Similar analyses would help to deepen the understanding of extreme impacts from spatially dependent river floods (Berghuijs et al., 2019; Jongman et al., 2014; Kemter et al., 2020), which may intensify in the future due to the larger spatial-footprints of rainfall extremes (Bevacqua et al., 2021), or continental scale renewable energy shortages driven by large scale high pressure systems (Van der Wiel, Stoop, et al., 2019). At the regional scale, relevant events include widespread storm surges (Enríquez et al., 2020) and multiple wildfires (Portier et al., 2017) such as those in California in 2017 (Balch et al., 2020), which can deplete response capacity, resulting in extreme losses.
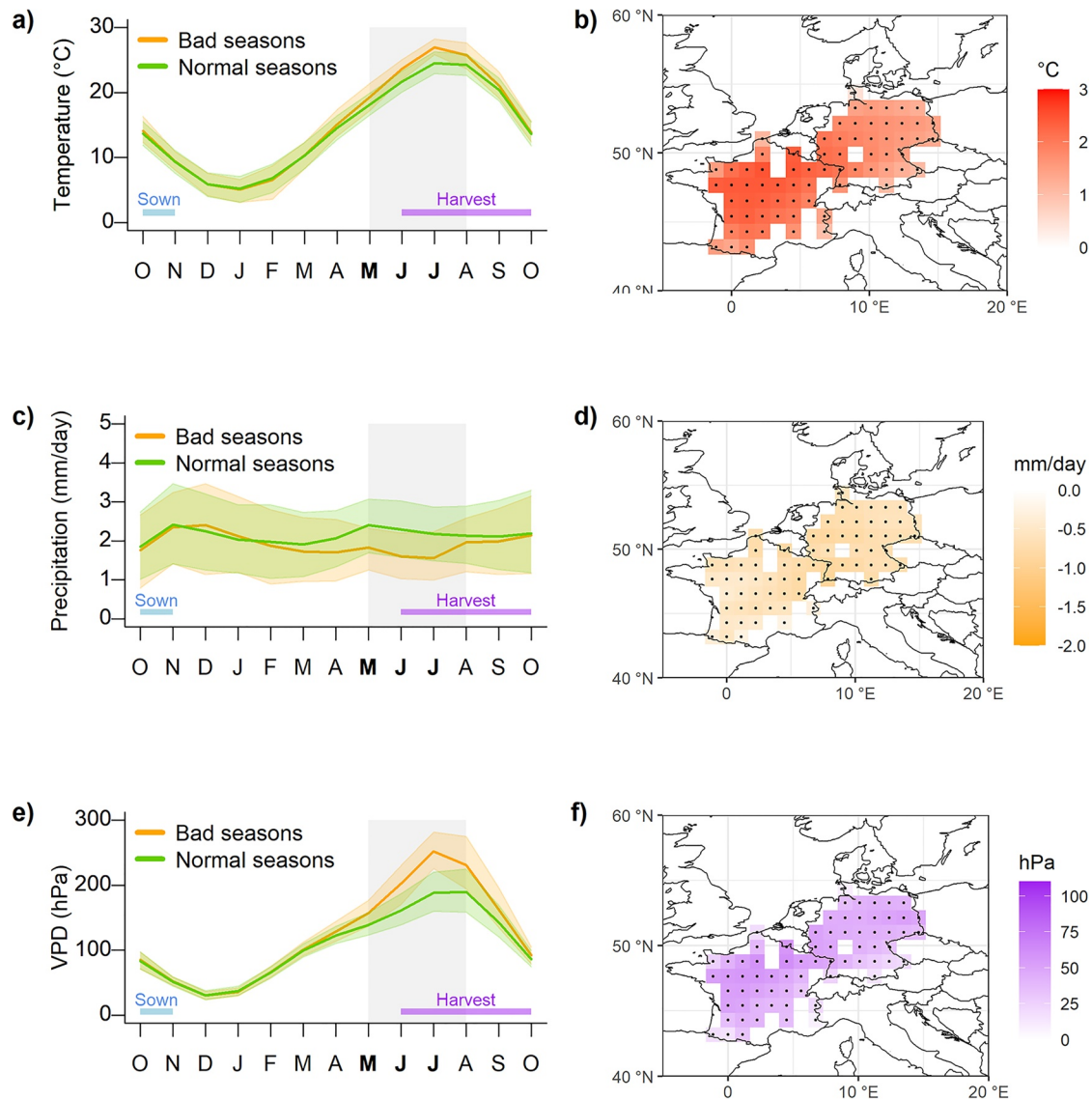
Figure 10. Temporal and spatial composites of potential meteorological drivers of growing seasons leading to concurrent crop failure in Germany and France (bad seasons, orange) and all other seasons (green). (a and b) maximum temperature; (c and d) precipitation; (e and f) vapor-pressure deficit (VPD). Shading in (a, c and e) highlight the 80th percentile range of the considered growing seasons. Blue and purple horizontal bars indicate the range of sown and harvest dates over the considered area. Gray shading indicates the period May-July considered for the composite on the right panels. Stippling in (b, d and f) indicates statistically significant differences at the 5% significance level based on a *t*-test.

6. Discussion and Conclusions

Building on the recently introduced typology of compound events (Zscheischler et al., 2020), in this work we provide guidelines for the study of a set of highly heterogeneous compound events. These guidelines are applicable to events that might differ from the ones analyzed here (e.g., belonging to very different impact domains, such as geological system and insurance industries), but have similar causal structure. For example, the approaches that were presented to study clustering and associated impacts can be useful for analyzing both landslides and insurance losses, where the former may be caused by clustered heavy precipitation events and the latter by clustered windstorms. Using our typology-based selection of case studies we highlight six recommendations that are common to the study of the four different types of compound events.

1. Causal diagrams (e.g., Figure 1) provide a simple but rigorous tool (Pearl & Mackenzie, 2018) that offers a common language to meet the challenges of representing, discussing, and communicating relevant compounding mechanisms among experts of different disciplines (Leonard et al., 2014; Lloyd & Shepherd, 2020).

2. From a methodological point of view, our results highlight the relevance of considering univariate impact indicators in compound event studies (here, the Leaf Area Index (LAI) for the vegetation impacts, water level for flooding, landslide occurrences, and aggregated crop yields). Such an *impact-centric* approach allows for a backward analysis to identify relevant hazards and drivers of the considered impacts, hence guaranteeing a focused analysis on impactful combinations of drivers (Bevacqua et al., 2017; Van der Wiel et al., 2020; Zscheischler et al., 2014). When impact data are not available, expert knowledge is required to define impact proxies or potentially impactful multivariate drivers.

3. Composites of climatic conditions (Figures 2, 5 and 10) associated with impacts provide a simple but useful tool to gain a first-hand understanding of the potential drivers of impacts. Nevertheless, to avoid running the risk of associating spurious correlations with causation, composites should be interpreted carefully based on expert knowledge and/or combined with advanced process-based modeling to test causal hypothesizes via, for example, counterfactual experiments or causal inference (Bastos et al., 2020; Runge, Bathiany, et al., 2019). For example, anomalies in the composites of time series in Figure 10 are correlated, hence disentangling causal effects on crop yields requires additional modeling, e.g., based on advanced statistical methods (Runge, Nowack, et al., 2019).

4. Advanced physically based models, such as crop and hydrodynamical flooding models, are important for studying the dynamics of many compound events, especially under climate change conditions. In fact, simple statistical models, such as regression, may not provide accurate information about future changes that are outside the observational range, and more sophisticated approaches from extreme value theory are required (Engelke & Ivanovs, 2021).

5. Compound event occurrence probabilities and their future changes can be highly uncertain due to combined uncertainties in multiple drivers and associated interplay (Bevacqua, Vousdoukas, Zappa, et al., 2020; Santos et al., 2021; Villalobos-Herrera et al., 2021). In this context, event-based storylines, which explore consequences of high-impact plausible events either or both under present and future climates putting emphasis on plausibility rather than probability, can provide very effective information for improving emergency preparedness to compound events (Sillmann et al., 2021).

6. The separation between compound event types is not clear-cut and soft boundaries exist between them (Zscheischler et al., 2020). For example, *multivariate* compound coastal flooding may be affected by *temporally compounding* features since high river discharge can be caused by precipitation from multiple storms in a quick succession (Bevacqua, Vousdoukas, Shepherd, & Vrac, 2020; Ward et al., 2018) (Figure 3). Hence, methods specifically useful for studying different types of compound events can sometimes be combined. Importantly, our case studies highlight that, depending on the research question of interest, a user will typically focus on a specific *compound feature*, for example the multivariate feature of compound flooding from ocean and riverine processes, and therefore ultimately employ tools that are useful for the compound feature of interest.

Given the complexity and diversity of compound events, each event is different and therefore our recommendations are somewhat dependent on the selected case studies. Follow-up work could expand and generalize the presented guidelines, for instance by considering different compound events and different research questions (e.g., attributing compound events to anthropogenic climate change, Zscheischler and Lehner, 2021) and in this way provide additional insights to advance the analysis of different compound event types. Furthermore, creating an inventory of methods that are useful for analyzing different types of compound events would be particularly helpful to users in order to identify appropriate analysis tools that can address specific research questions of interest. Given the extreme impacts often caused by different types of compound events, this study is a step toward the development of fundamental guidelines for incorporating a compound event perspective across disciplines and sectors for improved process understanding and risk assessments.

Data Availability Statement

Leaf Area Index (LAI) data is available at https://www.ncei.noaa.gov/access/metadata/landing-page/bin/iso?id=gov.noaa.ncdc:C00898. The ESA-CCI Land cover data set is available through the copernicus C3S at https://cds.climate.copernicus.eu/cdsapp#!/dataset/satellite-land-cover?tab=overview. ERA5 reanalysis is available through Hersbach et al. (2020) at https://climate.copernicus.eu/climate-reanalysis. Water levels used in the compound flooding analysis are available on request from the Australian Bureau of Meteorology (http://www.bom.gov.au/), the Department of Transport (https://www.transport.wa.gov.au/) and the Department of Water and Environmental Regulation (https://www.der.wa.gov.au/) in Western Australia. The landslide data set is provided in Zêzere et al. (2015). The IBERIA02 precipitation data set is available through Belo-Pereira et al. (2011) at https://www.ipma.pt/pt/produtoseservicos/index.jsp?page=dataset.pt02.xml&print=true. The climate and associated crop simulations are available through Ribeiro et al. (2021) at http://doi.org/10.5281/zenodo.5113280.

References

Anderegg, W. R. L., Trugman, A. T., Badgley, G., Konings, A. G., & Shaw, J. (2020). Divergent forest sensitivity to repeated extreme droughts. *Nature Climate Change*, *10*(12), 1091–1095. https://doi.org/10.1038/s41558-020-00919-1

Anderson, W. B., Seager, R., Baethgen, W., Cane, M., & You, L. (2019). Synchronous crop failures and climate-forced production variability. *Science Advances*, *5*(7), eaaw1976. https://doi.org/10.1126/sciadv.aaw1976

Balch, J. K., Iglesias, V., Braswell, A. E., Rossi, M. W., Joseph, M. B., Mahood, A. L., & Travis, W. R. (2020). Social-environmental extremes: Rethinking extraordinary events as outcomes of interacting biophysical and social systems. *Earth's Future*, *8*(7), e2019EF001319. https://doi.org/10.1029/2019ef001319

Baldwin, J. W., Dessy, J. B., Vecchi, G. A., & Oppenheimer, M. (2019). Temporally compound heat wave events and global warming: An emerging hazard. *Earth's Future*, *7*(4), 411–427. https://doi.org/10.1029/2018ef000989

Barton, Y., Giannakaki, P., von Waldow, H., Chevalier, C., Pfahl, S., & Martius, O. (2016). Clustering of regional-scale extreme precipitation events in southern Switzerland. *Monthly Weather Review*, *144*(1), 347–369. https://doi.org/10.1175/mwr-d-15-0205.1

Bastos, A., Ciais, P., Friedlingstein, P., Sitch, S., Pongratz, J., Fan, L., & Zaehle, S. (2020). Direct and seasonal legacy effects of the 2018 heat wave and drought on European ecosystem productivity. *Science Advances*, *6*(24), eaba2724. https://doi.org/10.1126/sciadv.aba2724

Bastos, A., Gouveia, C. M., Trigo, R. M., & Running, S. W. (2014). Analysing the spatio-temporal impacts of the 2003 and 2010 extreme heatwaves on plant productivity in Europe. *Biogeosciences*, *11*(13), 3421–3435. https://doi.org/10.5194/bg-11-3421-2014

Beillouin, D., Schauberger, B., Bastos, A., Ciais, P., & Makowski, D. (2020). Impact of extreme weather conditions on European crop production in 2018. *Philosophical Transactions of the Royal Society B: Biological Sciences*, *375*(1810), 0510. https://doi.org/10.1098/rstb.2019.0510

Belo-Pereira, M., Dutra, E., & Viterbo, P. (2011). Evaluation of global precipitation data sets over the Iberian Peninsula. *Journal of Geophysical Research*, *116*, D20101. https://doi.org/10.1029/2010JD015481

Ben-Ari, T., Boé, J., Ciais, P., Lecerf, R., der Velde, M. V., & Makowski, D. (2018). Causes and implications of the unforeseen 2016 extreme yield loss in the breadbasket of France. *Nature Communications*, *9*(1). https://doi.org/10.1038/s41467-018-04087-x

Berghuijs, W. R., Allen, S. T., Harrigan, S., & Kirchner, J. W. (2019). Growing spatial scales of synchronous river flooding in Europe. *Geophysical Research Letters*, *46*(3), 1423–1428. https://doi.org/10.1029/2018gl081883

Berghuijs, W. R., Woods, R. A., Hutton, C. J., & Sivapalan, M. (2016). Dominant flood generating mechanisms across the United States. *Geophysical Research Letters*, *43*(9), 4382–4390. https://doi.org/10.1002/2016gl068070

Bermúdez, M., Cea, L., & Sopelana, J. (2019). Quantifying the role of individual flood drivers and their correlations in flooding of coastal river reaches. *Stochastic Environmental Research and Risk Assessment*, *33*(10), 1851–1861. https://doi.org/10.1007/s00477-019-01733-8

Bevacqua, E., Maraun, D., Hobæk Haff, I., Widmann, M., & Vrac, M. (2017). Multivariate statistical modelling of compound events via pair-copula constructions: Analysis of floods in Ravenna (Italy). *Hydrology and Earth System Sciences*, *21*(6), 2701–2723. https://doi.org/10.5194/hess-21-2701-2017

Bevacqua, E., Maraun, D., Vousdoukas, M. I., Voukouvalas, E., Vrac, M., Mentaschi, L., & Widmann, M. (2019). Higher probability of compound flooding from precipitation and storm surge in Europe under anthropogenic climate change. *Science Advances*, *5*(9). eaaw5531. https://doi.org/10.1126/sciadv.aaw5531

Bevacqua, E., Shepherd, T. G., Watson, P. A., Sparrow, S., Wallom, D., & Mitchell, D. (2021). Larger spatial footprint of wintertime total precipitation extremes in a warmer climate. *Geophysical Research Letters*, *48*(8), e2020GL091990. https://doi.org/10.1029/2020gl091990

Bevacqua, E., Vousdoukas, M. I., Shepherd, T. G., & Vrac, M. (2020). Brief communication: The role of using precipitation or river discharge data when assessing global coastal compound flooding. *Natural Hazards and Earth System Sciences*, *20*(6), 1765–1782. https://doi.org/10.5194/nhess-20-1765-2020

Bevacqua, E., Vousdoukas, M. I., Zappa, G., Hodges, K., Shepherd, T. G., Maraun, D., et al. (2020). More meteorological events that drive compound coastal flooding are projected under climate change. *Communications Earth & Environment*, *1*(47). https://doi.org/10.1038/s43247-020-00044-z

Bevacqua, E., Zappa, G., & Shepherd, T. G. (2020). Shorter cyclone clusters modulate changes in European wintertime precipitation extremes. *Environmental Research Letters*, *15*, 124005. https://doi.org/10.1088/1748-9326/abbde7

Bilskie, M. V., & Hagen, S. C. (2018). Defining flood zone transitions in low-gradient coastal regions. *Geophysical Research Letters*, *45*(6), 2761–2770. https://doi.org/10.1002/2018gl077524

Brunetti, M. T., Peruccacci, S., Rossi, M., Luciani, S., Valigi, D., & Guzzetti, F. (2010). Rainfall thresholds for the possible occurrence of landslides in Italy. *Natural Hazards and Earth System Sciences*, *10*(3), 447–458. https://doi.org/10.5194/nhess-10-447-2010

Buermann, W., Forkel, M., O'sullivan, M., Sitch, S., Friedlingstein, P., Haverd, V., et al. (2018). Widespread seasonal compensation effects of spring warming on northern plant productivity. *Nature*, *562*(7725), 110–114. https://doi.org/10.1038/s41586-018-0555-7

Chauhan, T., & Ghosh, S. (2020). Partitioning of memory and real-time connections between variables in Himalayan ecohydrological process networks. *Journal of Hydrology*, *590*, 125434. https://doi.org/10.1016/j.jhydrol.2020.125434

Claverie, M., Matthews, J., Vermote, E., & Justice, C. (2016). A 30+ year AVHRR LAI and FAPAR climate data record: Algorithm description and validation. *Remote Sensing*, *8*(3), 263. https://doi.org/10.3390/rs8030263

COGECA, C. (2003). *Assessment of the impact of the heat wave and drought of the summer 2003 on agriculture and forestry*. Committee of Agricultural Organisations in the European Union and General Committee for Agricultural Cooperation in the European Union.

Couasnon, A., Eilander, D., Muis, S., Veldkamp, T. I., Haigh, I. D., Wahl, T., et al. (2020). Measuring compound flood potential from river discharge and storm surge extremes at the global scale. *Natural Hazards and Earth System Sciences*, *20*(2), 489–504. https://doi.org/10.5194/nhess-20-489-2020

Dacre, H. F., & Pinto, J. G. (2020). Serial clustering of extratropical cyclones: A review of where, when and why it occurs. *NPJ Climate and Atmospheric Science*, *3*(1). https://doi.org/10.1038/s41612-020-00152-9

de Brum Ferreira, A., & Zêzere, J. L. (1997). Portugal and the Portuguese Atlantic islands. In *Geomorphological hazards of Europe* (pp. 391–407). Elsevier. https://doi.org/10.1016/s0928-2025(97)80017-x

Deser, C., Lehner, F., Rodgers, K. B., Ault, T., Delworth, T. L., DiNezio, P. N., et al. (2020). Insights from Earth system model initial-condition large ensembles and future prospects. *Nature Climate Change*, *10*(4), 277–286. https://doi.org/10.1038/s41558-020-0731-2

Eilander, D., Couasnon, A., Ikeuchi, H., Muis, S., Yamazaki, D., Winsemius, H. C., & Ward, P. J. (2020). The effect of surge on riverine flood hazard and impact in deltas globally. *Environmental Research Letters*, *15*(10), 104007. https://doi.org/10.1088/1748-9326/ab8ca6

Eliot, M. (2012). Sea level variability influencing coastal flooding in the swan river region, Western Australia. *Continental Shelf Research*, *33*, 14–28. https://doi.org/10.1016/j.csr.2011.08.012

Engelke, S., & Ivanovs, J. (2021). Sparse structures for multivariate extremes. *Annual Review of Statistics and Its Application*, *8*, 241–270. https://doi.org/10.1146/annurev-statistics-040620-041554

Enríquez, A. R., Wahl, T., Marcos, M., & Haigh, I. D. (2020). Spatial footprints of storm surges along the global coastlines. *Journal of Geophysical Research: Oceans*, *125*(9), e2020JC016367. https://doi.org/10.1029/2020jc016367

Evans, J., & Schreider, S. (2002). Hydrological impacts of climate change on inflows to Perth, Australia. *Climatic Change*, *55*(3), 361–393. https://doi.org/10.1023/a:1020588416541

Falco, S. D., Adinolfi, F., Bozzola, M., & Capitanio, F. (2014). Crop insurance as a strategy for adapting to climate change. *Journal of Agricultural Economics*, *65*(2), 485–504. https://doi.org/10.1111/1477-9552.12053

FAOSTAT. (2021). *FAO statistics*. Food and agriculture organization of the united nations.

Ferro, C. A. T., & Segers, J. (2003). Inference for clusters of extreme values. *Journal of the Royal Statistical Society: Series B (Statistical Methodology)*, *65*(2), 545–556. https://doi.org/10.1111/1467-9868.00401

Flach, M., Sippel, S., Gans, F., Bastos, A., Brenning, A., Reichstein, M., & Mahecha, M. D. (2018). Contrasting biosphere responses to hydrometeorological extremes: Revisiting the 2010 western Russian heatwave. *Biogeosciences*, *15*(20), 6067–6085. https://doi.org/10.5194/bg-15-6067-2018

Forkel, M., Thonicke, K., Beer, C., Cramer, W., Bartalev, S., & Schmullius, C. (2012). Extreme fire events are related to previous-year surface moisture conditions in permafrost-underlain larch forests of Siberia. *Environmental Research Letters*, *7*(4), 044021. https://doi.org/10.1088/1748-9326/7/4/044021

Froude, M. J., & Petley, D. N. (2018). Global fatal landslide occurrence from 2004 to 2016. *Natural Hazards and Earth System Sciences*, *18*(8), 2161–2181.

Ganguli, P., Paprotny, D., Hasan, M., Güntner, A., & Merz, B. (2020). Projected changes in compound flood hazard from riverine and coastal floods in Northwestern Europe. *Earth's Future*, *8*(11), e2020EF001752. https://doi.org/10.1029/2020ef001752

Gariano, S. L., Brunetti, M. T., Iovine, G., Melillo, M., Peruccacci, S., Terranova, O., et al. (2015). Calibration and validation of rainfall thresholds for shallow landslide forecasting in Sicily, Southern Italy. *Geomorphology*, *228*, 653–665. https://doi.org/10.1016/j.geomorph.2014.10.019

Gaupp, F., Hall, J., Hochrainer-Stigler, S., & Dadson, S. (2019). Changing risks of simultaneous global breadbasket failure. *Nature Climate Change*, *10*(1), 54–57. https://doi.org/10.1038/s41558-019-0600-z

Gori, A., Lin, N., & Xi, D. (2020). Tropical cyclone compound flood hazard assessment: From investigating drivers to quantifying extreme water levels. *Earth's Future*, *8*(12). https://doi.org/10.1029/2020ef001660

Gudmundsson, L., Rego, F. C., Rocha, M., & Seneviratne, S. I. (2014). Predicting above normal wildfire activity in southern Europe as a function of meteorological drought. *Environmental Research Letters*, *9*(8), 084008. https://doi.org/10.1088/1748-9326/9/8/084008

Guzzetti, F., Peruccacci, S., Rossi, M., & Stark, C. P. (2007). Rainfall thresholds for the initiation of landslides in central and southern Europe. *Meteorology and Atmospheric Physics*, *98*(3–4), 239–267. https://doi.org/10.1007/s00703-007-0262-7

Hao, Z., Hao, F., Xia, Y., Singh, V. P., & Zhang, X. (2019). A monitoring and prediction system for compound dry and hot events. *Environmental Research Letters*, *14*(11), 114034. https://doi.org/10.1088/1748-9326/ab4df5

Hazeleger, W., Severijns, C., Semmler, T., Ştefănescu, S., Yang, S., Wang, X., et al. (2010). EC-Earth: A seamless Earth-system prediction approach in action. *Bulletin of the American Meteorological Society*, *91*(10), 1357–1364. https://doi.org/10.1175/2010bams2877.1

Hazeleger, W., Van den Hurk, B., Min, E., Van Oldenborgh, G., Petersen, A., Stainforth, D., et al. (2015). Tales of future weather. *Nature Climate Change*, *5*(2), 107–113. https://doi.org/10.1038/nclimate2450

Helaire, L. T., Talke, S. A., Jay, D. A., & Chang, H. (2020). Present and future flood hazard in the lower Columbia River estuary: Changing flood hazards in the Portland-Vancouver metropolitan area. *Journal of Geophysical Research: Oceans*, *125*(7), e2019JC015928. https://doi.org/10.1029/2019jc015928

Hendry, A., Haigh, I. D., Nicholls, R. J., Winter, H., Neal, R., Wahl, T., et al. (2019). Assessing the characteristics and drivers of compound flooding events around the UK coast. *Hydrology and Earth System Sciences*, *23*(7), 3117–3139. https://doi.org/10.5194/hess-23-3117-2019

Hénin, R., Ramos, A. M., Pinto, J. G., & Liberato, M. L. R. (2021). A ranking of concurrent precipitation and wind events for the Iberian Peninsula. *International Journal of Climatology*, *41*(2), 1421–1437. https://doi.org/10.1002/joc.6829

Hersbach, H., Bell, B., Berrisford, P., Hirahara, S., Horányi, A., Muñoz-Sabater, J., et al. (2020). The ERA5 global reanalysis. *Quarterly Journal of the Royal Meteorological Society*, *146*(730), 1999–2049. https://doi.org/10.1002/qj.3803

Hillier, J. K., & Dixon, R. S. (2020). Seasonal impact-based mapping of compound hazards. *Environmental Research Letters*, *15*(11), 114013. https://doi.org/10.1088/1748-9326/abbc3d

Hillier, J. K., Macdonald, N., Leckebusch, G. C., & Stavrinides, A. (2015). Interactions between apparently 'primary' weather-driven hazards and their cost. *Environmental Research Letters*, *10*(10), 104003. https://doi.org/10.1088/1748-9326/10/10/104003

Hillier, J. K., Matthews, T., Wilby, R. L., & Murphy, C. (2020). Multi-hazard dependencies can increase or decrease risk. *Nature Climate Change*, *10*(7), 595–598. https://doi.org/10.1038/s41558-020-0832-y

Hirabayashi, Y., Mahendran, R., Koirala, S., Konoshima, L., Yamazaki, D., Watanabe, S., et al. (2013). Global flood risk under climate change. *Nature Climate Change*, *3*(9), 816–821. https://doi.org/10.1038/nclimate1911

Hoegh-Guldberg, O., Jacob, D., Bindi, M., Brown, S., Camilloni, I., Diedhiou, A., & Zhou, G. (2018). *Impacts of 1.5°C global warming on natural and human systems Global warming of 1.5°C. An IPCC Special Report.*

Hoerling, M., Kumar, A., Dole, R., Nielsen-Gammon, J. W., Eischeid, J., Perlwitz, J., et al. (2013). Anatomy of an extreme event. *Journal of Climate*, *26*(9), 2811–2832. https://doi.org/10.1175/jcli-d-12-00270.1

Hope, P., Abbs, D., Bhend, J., Chiew, F., Church, J., Ekström, M., & McInnes, K. (2015). Southern and south-western flatlands cluster report. In *Climate change in Australia: Projections for Australia's natural resource management regions*. CSIRO and Bureau of Meteorology, Australia. Retrieved From https://www.climatechangeinaustralia.gov.au/media/ccia/2.1

Iverson, R. M. (2000). Landslide triggering by rain infiltration. *Water Resources Research*, *36*(7), 1897–1910. https://doi.org/10.1029/2000wr900090

James, G., Witten, D., Hastie, T., & Tibshirani, R. (2013). Introduction. In *Springer texts in statistics* (pp. 1–14). Springer. https://doi.org/10.1007/978-1-4614-7138-7_1

Jézéquel, A., Bevacqua, E., d'Andrea, F., Thao, S., Vautard, R., Vrac, M., & Yiou, P. (2020). Conditional and residual trends of singular hot days in Europe. *Environmental Research Letters*, *15*(6), 064018. https://doi.org/10.1088/1748-9326/ab76dd

Jiang, Q., Li, W., Fan, Z., He, X., Sun, W., Chen, S., et al. (2021). Evaluation of the ERA5 reanalysis precipitation dataset over Chinese Mainland. *Journal of Hydrology*, *595*, 125660. https://doi.org/10.1016/j.jhydrol.2020.125660

Jongman, B. (2018). Effective adaptation to rising flood risk. *Nature Communications*, *9*(1), 1–3. https://doi.org/10.1038/s41467-018-04396-1

Jongman, B., Hochrainer-Stigler, S., Feyen, L., Aerts, J. C. J. H., Mechler, R., Botzen, W. J. W., et al. (2014). Increasing stress on disaster-risk finance due to large floods. *Nature Climate Change*, *4*(4), 264–268. https://doi.org/10.1038/nclimate2124

Kemter, M., Merz, B., Marwan, N., Vorogushyn, S., & Blöschl, G. (2020). Joint trends in flood magnitudes and spatial extents across Europe. *Geophysical Research Letters*, *47*(7), e2020GL087464. https://doi.org/10.1029/2020gl087464

Khanam, M., Sofia, G., Koukoula, M., Lazin, R., Nikolopoulos, E. I., Shen, X., & Anagnostou, E. N. (2021). Impact of compound flood event on coastal critical infrastructures considering current and future climate. *Natural Hazards and Earth System Sciences*, *21*(2), 587–605. https://doi.org/10.5194/nhess-21-587-2021

Khojasteh, D., Glamore, W., Heimhuber, V., & Felder, S. (2021). Sea level rise impacts on estuarine dynamics: A review. *Science of the Total Environment*, *780*, 146470. https://doi.org/10.1016/j.scitotenv.2021.146470

Klerk, W. -J., Winsemius, H., van Verseveld, W., Bakker, A., & Diermanse, F. (2015). The co-incidence of storm surges and extreme discharges within the Rhine–Meuse Delta. *Environmental Research Letters*, *10*(3), 035005. https://doi.org/10.1088/1748-9326/10/3/035005

Kornhuber, K., Coumou, D., Vogel, E., Lesk, C., Donges, J. F., Lehmann, J., & Horton, R. M. (2019). Amplified Rossby waves enhance risk of concurrent heatwaves in major breadbasket regions. *Nature Climate Change*, *10*(1), 48–53. https://doi.org/10.1038/s41558-019-0637-z

Kumbier, K., Carvalho, R. C., Vafeidis, A. T., & Woodroffe, C. D. (2018). Investigating compound flooding in an estuary using hydrodynamic modelling: A case study from the Shoalhaven River, Australia. *Natural Hazards and Earth System Sciences*, *18*(2), 463–477. https://doi.org/10.5194/nhess-18-463-2018

Leonard, M., Westra, S., Phatak, A., Lambert, M., van den Hurk, B., McInnes, K., et al. (2014). A compound event framework for understanding extreme impacts. *Wiley Interdisciplinary Reviews: Climate Change*, *5*(1), 113–128. https://doi.org/10.1002/wcc.252

Lian, X., Piao, S., Li, L. Z. X., Li, Y., Huntingford, C., Ciais, P., & McVicar, T. R. (2020). Summer soil drying exacerbated by earlier spring greening of northern vegetation. *Science Advances*, *6*(1). eaax0255. https://doi.org/10.1126/sciadv.aax0255

Lloyd, E. A., & Shepherd, T. G. (2020). Environmental catastrophes, climate change, and attribution. *Annals of the New York Academy of Sciences*, *1469*(1), 105–124. https://doi.org/10.1111/nyas.14308

Mandrekar, J. N. (2010). Receiver operating characteristic curve in diagnostic test assessment. *Journal of Thoracic Oncology*, *5*(9), 1315–1316. https://doi.org/10.1097/jto.0b013e3181ec173d

Martius, O., Pfahl, S., & Chevalier, C. (2016). A global quantification of compound precipitation and wind extremes. *Geophysical Research Letters*, *43*(14), 7709–7717. https://doi.org/10.1002/2016gl070017

Matthews, T., Wilby, R. L., & Murphy, C. (2019). An emerging tropical cyclone–deadly heat compound hazard. *Nature Climate Change*, *9*(8), 602–606. https://doi.org/10.1038/s41558-019-0525-6

Mehrabi, Z., & Ramankutty, N. (2019). Synchronized failure of global crop production. *Nature Ecology & Evolution*, *3*(5), 780–786. https://doi.org/10.1038/s41559-019-0862-x

Messori, G., Bevacqua, E., Caballero, R., Coumou, D., De Luca, P., Faranda, D., et al. (2021). Compound climate events and extremes in the midlatitudes: Dynamics, simulation, and statistical characterization. *Bulletin of the American Meteorological Society*, *102*(4), E774–E781. https://doi.org/10.1175/bams-d-20-0289.1

Mitchell-Wallace, K., Jones, M., Hillier, J., & Foote, M. (2017). *Natural catastrophe risk management and modelling: A practitioner's guide*. John Wiley & Sons.

Moftakhari, H. R., Salvadori, G., AghaKouchak, A., Sanders, B. F., & Matthew, R. A. (2017). Compounding effects of sea level rise and fluvial flooding. *Proceedings of the National Academy of Sciences*, *114*(37), 9785–9790. https://doi.org/10.1073/pnas.1620325114

Mohanty, M. P., Sherly, M. A., Ghosh, S., & Karmakar, S. (2020). Tide-rainfall flood quotient: An incisive measure of comprehending a region's response to storm-tide and pluvial flooding. *Environmental Research Letters*, *15*(6), 064029. https://doi.org/10.1088/1748-9326/ab8092

Nogueira, M. (2020). Inter-comparison of ERA-5, ERA-interim and GPCP rainfall over the last 40 years: Process-based analysis of systematic and random differences. *Journal of Hydrology*, *583*, 124632. https://doi.org/10.1016/j.jhydrol.2020.124632

Olbert, A. I., Comer, J., Nash, S., & Hartnett, M. (2017). High-resolution multi-scale modelling of coastal flooding due to tides, storm surges and rivers inflows. A cork city example. *Coastal Engineering*, *121*, 278–296. https://doi.org/10.1016/j.coastaleng.2016.12.006

Parker, K., Ruggiero, P., Serafin, K. A., & Hill, D. F. (2019). Emulation as an approach for rapid estuarine modeling. *Coastal Engineering*, *150*, 79–93. https://doi.org/10.1016/j.coastaleng.2019.03.004

Pearl, J., & Mackenzie, D. (2018). *The book of why: The new science of cause and effect*. Penguin Books.

Pereira, S., Santos, P., Zêzere, J., Tavares, A., Garcia, R., & Oliveira, S. (2020). A landslide risk index for municipal land use planning in Portugal. *Science of the Total Environment*, *735*, 139463. https://doi.org/10.1016/j.scitotenv.2020.139463

Peruccacci, S., Brunetti, M. T., Gariano, S. L., Melillo, M., Rossi, M., & Guzzetti, F. (2017). Rainfall thresholds for possible landslide occurrence in Italy. *Geomorphology*, *290*, 39–57. https://doi.org/10.1016/j.geomorph.2017.03.031

Petley, D. (2012). Global patterns of loss of life from landslides. *Geology*, *40*(10), 927–930.

Portier, J., Gauthier, S., Robitaille, A., & Bergeron, Y. (2017). Accounting for spatial autocorrelation improves the estimation of climate, physical environment and vegetation's effects on boreal forest's burn rates. *Landscape Ecology*, *33*(1), 19–34. https://doi.org/10.1007/s10980-017-0578-8

Postance, B., Hillier, J., Dijkstra, T., & Dixon, N. (2018). Comparing threshold definition techniques for rainfall-induced landslides: A national assessment using radar rainfall. *Earth Surface Processes and Landforms*, *43*(2), 553–560. https://doi.org/10.1002/esp.4202

Priestley, M. D., Dacre, H. F., Shaffrey, L. C., Hodges, K. I., & Pinto, J. G. (2018). The role of serial European windstorm clustering for extreme seasonal losses as determined from multi-centennial simulations of high-resolution global climate model data. *Natural Hazards and Earth System Sciences*, *18*(11), 2991–3006. https://doi.org/10.5194/nhess-18-2991-2018

Priestley, M. D., Pinto, J. G., Dacre, H. F., & Shaffrey, L. C. (2017). The role of cyclone clustering during the stormy winter of 2013/2014. *Weather*, *72*(7), 187–192. https://doi.org/10.1002/wea.3025

Ramos, A. M., Trigo, R. M., & Liberato, M. L. (2014). A ranking of high-resolution daily precipitation extreme events for the Iberian Peninsula. *Atmospheric Science Letters*, *15*(4), 328–334. https://doi.org/10.1002/asl2.507

Ramos, A. M., Trigo, R. M., Liberato, M. L., & Tomé, R. (2015). Daily precipitation extreme events in the Iberian Peninsula and its association with atmospheric rivers. *Journal of Hydrometeorology*, *16*(2), 579–597. https://doi.org/10.1175/jhm-d-14-0103.1

Ray, D. K., Gerber, J. S., MacDonald, G. K., & West, P. C. (2015). Climate variation explains a third of global crop yield variability. *Nature Communications*, *6*(1). https://doi.org/10.1038/ncomms6989

Raymond, C., Horton, R. M., Zscheischler, J., Martius, O., AghaKouchak, A., Balch, J., et al. (2020). Understanding and managing connected extreme events. *Nature Climate Change*, *10*(7), 611–621. https://doi.org/10.1038/s41558-020-0790-4

Ribeiro, A. F. S., Russo, A., Gouveia, C. M., Páscoa, P., & Zscheischler, J. (2020). Risk of crop failure due to compound dry and hot extremes estimated with nested copulas. *Biogeosciences*, *17*(19), 4815–4830. https://doi.org/10.5194/bg-17-4815-2020

Ribeiro, A. F. S., Vignotto, E., Van der Wiel, K., Zhang, T., Rivoire, P., Bevacqua, E., & Zscheischler, J. (2021). *A large-ensemble simulation of yields and meteorological drivers to evaluate spatial compounding crop failures in Europe*[Data set]. Zenodo. https://doi.org/10.5281/zenodo.5113280

Rivoire, P., Martius, O., & Naveau, P. (2021). A comparison of moderate and extreme ERA-5 daily precipitation with two observational data sets. *Earth and Space Science*, *8*(4), e2020EA001633. https://doi.org/10.1029/2020ea001633

Ruiter, M. C., Couasnon, A., Homberg, M. J. C., Daniell, J. E., Gill, J. C., & Ward, P. J. (2020). Why we can no longer ignore consecutive disasters. *Earth's Future*, *8*(3). https://doi.org/10.1029/2019ef001425

Runge, J., Bathiany, S., Bollt, E., Camps-Valls, G., Coumou, D., Deyle, E., et al. (2019). Inferring causation from time series in Earth system sciences. *Nature Communications*, *10*(1), 2553. https://doi.org/10.1038/s41467-019-10105-3

Runge, J., Nowack, P., Kretschmer, M., Flaxman, S., & Sejdinovic, D. (2019). Detecting and quantifying causal associations in large nonlinear time series datasets. *Science Advances*, *5*(11), eaau4996. https://doi.org/10.1126/sciadv.aau4996

Santoro, M., Kirches, G., Wevers, J., Boettcher, M., Brockmann, C., Lamarche, C., & Defourny, P. (2017). *Land cover CCI: Product user guide version 2.0*. Climate Change Initiative Belgium.

Santos, V. M., Casas-Prat, M., Poschlod, B., Ragno, E., van den Hurk, B., Hao, Z., et al. (2021). Statistical modelling and climate variability of compound surge and precipitation events in a managed water system: A case study in the Netherlands. *Hydrology and Earth System Sciences*, *25*(6), 3595–3615. https://doi.org/10.5194/hess-25-3595-2021

Schepsmeier, U., Stoeber, J., Brechmann, E. C., Graeler, B., Nagler, T., & Erhardt, T. (2016). *VineCopula: Statistical inference of vine copulas. R package version*.

Schulzweida, U., Kornblueh, L., & Quast, R. (2006). Cdo user's guide. *Climate data operators*, *1*(6), 205–209.

Sebastian, A., Gori, A., Blessing, R. B., van der Wiel, K., & Bass, B. (2019). Disentangling the impacts of human and environmental change on catchment response during Hurricane Harvey. *Environmental Research Letters*, *14*(12), 124023. https://doi.org/10.1088/1748-9326/ab5234

Shepherd, T. G. (2019). Storyline approach to the construction of regional climate change information. *Proceedings of the Royal Society A*, *475*(2225), 0013. https://doi.org/10.1098/rspa.2019.0013

Sillmann, J., Shepherd, T. G., van den Hurk, B., Hazeleger, W., Martius, O., Slingo, J., & Zscheischler, J. (2021). Event-based storylines to address climate risk. *Earth's Future*, *9*(2). https://doi.org/10.1029/2020ef001783

Sopelana, J., Cea, L., & Ruano, S. (2018). A continuous simulation approach for the estimation of extreme flood inundation in coastal river reaches affected by meso- and macrotides. *Natural Hazards*, *93*(3), 1337–1358. https://doi.org/10.1007/s11069-018-3360-6

Swan River Trust. (2007). *Potential impacts of climate change on the Swan and Canning rivers*. Swan River Trust.

Tarek, M., Brissette, F. P., & Arsenault, R. (2020). Evaluation of the ERA5 reanalysis as a potential reference dataset for hydrological modelling over North America. *Hydrology and Earth System Sciences*, *24*(5), 2527–2544. https://doi.org/10.5194/hess-24-2527-2020

Teuling, A. J., Seneviratne, S. I., Stöckli, R., Reichstein, M., Moors, E., Ciais, P., et al. (2010). Contrasting response of European forest and grassland energy exchange to heatwaves. *Nature Geoscience*, *3*(10), 722–727. https://doi.org/10.1038/ngeo950

Thompson, V., Dunstone, N. J., Scaife, A. A., Smith, D. M., Slingo, J. M., Brown, S., & Belcher, S. E. (2017). High risk of unprecedented UK rainfall in the current climate. *Nature Communications*, *8*(1), 1–6. https://doi.org/10.1038/s41467-017-00275-3

Toreti, A., Belward, A., Perez-Dominguez, I., Naumann, G., Luterbacher, J., Cronie, O., et al. (2019). The exceptional 2018 European water seesaw calls for action on adaptation. *Earth's Future*, *7*(6), 652–663. https://doi.org/10.1029/2019ef001170

Van der Wiel, K., Lenderink, G., & de Vries, H. (2021). Physical storylines of future European drought events like 2018 based on ensemble climate modelling. *Weather and Climate Extremes*, *33*, 100350. https://doi.org/10.1016/j.wace.2021.100350

Van der Wiel, K., Selten, F. M., Bintanja, R., Blackport, R., & Screen, J. A. (2020). Ensemble climate-impact modelling: Extreme impacts from moderate meteorological conditions. *Environmental Research Letters*, *15*(3), 034050. https://doi.org/10.1088/1748-9326/ab7668

van der Wiel, K., Stoop, L., van Zuijlen, B., Blackport, R., van den Broek, M., & Selten, F. (2019). Meteorological conditions leading to extreme low variable renewable energy production and extreme high energy shortfall. *Renewable and Sustainable Energy Reviews*, *111*, 261–275. https://doi.org/10.1016/j.rser.2019.04.065

Van der Wiel, K., Wanders, N., Selten, F., & Bierkens, M. (2019). Added value of large ensemble simulations for assessing extreme river discharge in a 2°C warmer world. *Geophysical Research Letters*, *46*(4), 2093–2102. https://doi.org/10.1029/2019GL081967

Villalobos-Herrera, R., Bevacqua, E., Ribeiro, A. F., Auld, G., Crocetti, L., Mircheva, B., et al. (2021). Towards a compound-event-oriented climate model evaluation: A decomposition of the underlying biases in multivariate fire and heat stress hazards. *Natural Hazards and Earth System Sciences*, *21*(6), 1867–1885. https://doi.org/10.5194/nhess-21-1867-2021

Vogel, J., Rivoire, P., Deidda, C., Rahimi, L., Sauter, C. A., Tschumi, E., et al. (2021). Identifying meteorological drivers of extreme impacts: An application to simulated crop yields. *Earth System Dynamics*, *12*(1), 151–172. https://doi.org/10.5194/esd-12-151-2021

Vousdoukas, M. I., Mentaschi, L., Voukouvalas, E., Verlaan, M., Jevrejeva, S., Jackson, L. P., & Feyen, L. (2018). Global probabilistic projections of extreme sea levels show intensification of coastal flood hazard. *Nature Communications*, *9*(1), 2360. https://doi.org/10.1038/s41467-018-04692-w

Wahl, T., Jain, S., Bender, J., Meyers, S. D., & Luther, M. E. (2015). Increasing risk of compound flooding from storm surge and rainfall for major US cities. *Nature Climate Change*, *5*(12), 1093–1097. https://doi.org/10.1038/nclimate2736

Ward, P. J., Couasnon, A., Eilander, D., Haigh, I. D., Hendry, A., Muis, S., et al. (2018). Dependence between high sea-level and high river discharge increases flood hazard in global deltas and estuaries. *Environmental Research Letters*, *13*(8), 084012. https://doi.org/10.1088/1748-9326/aad400

Winsemius, H. C., Aerts, J., van Beek, L., Bierkens, M., Bouwman, A., Jongman, B., et al. (2016). Global drivers of future river flood risk. *Nature Climate Change*, *6*(4), 381–385. https://doi.org/10.1038/nclimate2893

Woo, G. (2021). A counterfactual perspective on compound weather risk. *Weather and Climate Extremes*, *32*, 100314. https://doi.org/10.1016/j.wace.2021.100314

Wu, W., Westra, S., & Leonard, M. (2021). Estimating the probability of compound floods in estuarine regions. *Hydrology and Earth System Sciences*, *25*(5), 2821–2841. https://doi.org/10.5194/hess-25-2821-2021

Zappa, G., & Shepherd, T. G. (2017). Storylines of atmospheric circulation change for European regional climate impact assessment. *Journal of Climate*, *30*(16), 6561–6577. https://doi.org/10.1175/jcli-d-16-0807.1

Zêzere, J. L., Pereira, S., Tavares, A. O., Bateira, C., Trigo, R. M., Quaresma, I., et al. (2014). DISASTER: A GIS database on hydro-geomorphologic disasters in Portugal. *Natural Hazards*, *72*(2), 503–532. https://doi.org/10.1007/s11069-013-1018-y

Zêzere, J. L., & Trigo, R. M. (2011). Impacts of the North Atlantic Oscillation on landslides. In *Advances in global change research* (pp. 199–212). Springer Netherlands. https://doi.org/10.1007/978-94-007-1372-7_14

Zêzere, J. L., Vaz, T., Pereira, S., Oliveira, S. C., Marques, R., & Garcia, R. A. C. (2015). Rainfall thresholds for landslide activity in portugal: A state of the art. *Environmental Earth Sciences*, *73*(6), 2917–2936. https://doi.org/10.1007/s12665-014-3672-0

Zhang, W., & Villarini, G. (2020). Deadly compound heat stress-flooding hazard across the central United States. *Geophysical Research Letters*, *47*(15), e2020GL089185. https://doi.org/10.1029/2020gl089185

Zhang, Y., Keenan, T. F., & Zhou, S. (2021). Exacerbated drought impacts on global ecosystems due to structural overshoot. *Nature Ecology & Evolution*, 1–9. https://doi.org/10.1038/s41559-021-01551-8

Zheng, B., Chenu, K., Doherty, A., & Chapman, S. (2014). *The APSIM-wheat module (7.5 R3008)*. Agricultural Production Systems Simulator (APSIM) Initiative.

Zscheischler, J., & Lehner, F. (2021). Attributing compound events to anthropogenic climate change. *Bulletin of the American Meteorological Society*, 1–45. https://doi.org/10.1175/bams-d-21-0116.1

Zscheischler, J., Martius, O., Westra, S., Bevacqua, E., Raymond, C., Horton, R., et al. (2020). A typology of compound weather and climate events. *Nature Reviews Earth & Environment*, *1*, 333–347. https://doi.org/10.1038/s43017-020-0060-z

Zscheischler, J., Michalak, A. M., Schwalm, C., Mahecha, M. D., Huntzinger, D. N., Reichstein, M., et al. (2014). Impact of large-scale climate extremes on biospheric carbon fluxes: An intercomparison based on MsTMIP data. *Global Biogeochemical Cycles*, *28*(6), 585–600. https://doi.org/10.1002/2014GB004826

Zscheischler, J., Orth, R., & Seneviratne, S. I. (2015). A submonthly database for detecting changes in vegetation-atmosphere coupling. *Geophysical Research Letters*, *42*(22), 9816–9824. https://doi.org/10.1002/2015gl066563

Zscheischler, J., Westra, S., Van Den Hurk, B. J., Seneviratne, S. I., Ward, P. J., Pitman, A., et al. (2018). Future climate risk from compound events. *Nature Climate Change*, *8*(6), 469–477. https://doi.org/10.1038/s41558-018-0156-3